

# Cellular and Mitochondrial Remodeling upon Defects in Iron-Sulfur Protein Biogenesis\*<sup>§</sup>

Received for publication, July 6, 2007, and in revised form, January 18, 2008. Published, JBC Papers in Press, January 28, 2008, DOI 10.1074/jbc.M705570200

Anja Hausmann<sup>‡</sup>, Birgit Samans<sup>§</sup>, Roland Lill<sup>‡</sup>, and Ulrich Mühlenhoff<sup>‡1</sup>

From the <sup>‡</sup>Institut für Zytobiologie und Zytopathologie, Philipps-Universität Marburg, Robert-Koch Strasse 6, 35032 Marburg and <sup>§</sup>Institut für Molekularbiologie und Tumorforschung, Emil-Mannkopf-Strasse 2, Philipps-Universität Marburg, 35032 Marburg, Germany

Biogenesis of iron-sulfur (Fe/S) proteins in eukaryotes is an essential process involving the mitochondrial iron-sulfur cluster (ISC) assembly and export machineries and the cytosolic iron/sulfur protein assembly (CIA) apparatus. To define the integration of Fe/S protein biogenesis into cellular homeostasis, we compared the global transcriptional responses to defects in the three biogenesis systems in *Saccharomyces cerevisiae* using DNA microarrays. Depletion of a member of the CIA machinery elicited only weak (up to 2-fold) alterations in gene expression with no clear preference for any specific cellular process. In contrast, depletion of components of the mitochondrial ISC assembly and export systems induced strong and largely overlapping transcriptional responses of more than 200 genes (2–100-fold changes). These alterations were strikingly similar, yet not identical, to the transcriptional profiles developed upon iron starvation. Hence, mitochondria and their ISC systems serve as primary physiological regulators exerting a global control of numerous iron-dependent processes. First, ISC depletion activates the iron-responsive transcription factors Aft1/2p leading to increased cellular iron acquisition. Second, respiration and heme metabolism are repressed ensuring the balanced utilization of iron by the two major iron-consuming processes, iron-sulfur protein and heme biosynthesis. Third, the decreased respiratory activity is compensated by induction of genes involved in glucose acquisition. Finally, transcriptional remodeling of the citric acid cycle and the biosyntheses of ergosterol and biotin reflect the iron dependence of these pathways. Together, our data suggest a model in which mitochondria perform a global regulatory role in numerous cellular processes linked to iron homeostasis.

Proteins with iron-sulfur (Fe/S) cofactors play important roles in fundamental cellular processes such as redox reactions, metabolic catalysis, and the regulation of gene expression

\* This work was supported by Deutsche Forschungsgemeinschaft Grants SFB 593 and TR1, the Gottfried-Wilhelm Leibniz Program, Grant GRK 1216, Fonds der Chemischen Industrie, Deutsches Humangenomprojekt, and the Fritz-Thyssen-Stiftung. The costs of publication of this article were defrayed in part by the payment of page charges. This article must therefore be hereby marked "advertisement" in accordance with 18 U.S.C. Section 1734 solely to indicate this fact.

Microarray data are available from ArrayExpress at EBI, accession number E-MEXP-1215.

<sup>§</sup> The on-line version of this article (available at <http://www.jbc.org>) contains supplemental Fig. S1, Tables SI–SIV, and additional references.

<sup>1</sup> To whom correspondence should be addressed. Tel.: 49-6421-2864171; Fax: 49-6421-2866414; E-mail: [muehlenh@staff.uni-marburg.de](mailto:muehlenh@staff.uni-marburg.de).

(1–3). In eukaryotes such as *Saccharomyces cerevisiae*, mitochondria play a central role in the biosynthesis of cellular Fe/S proteins (reviewed in Refs. 4–7). The mitochondrial matrix harbors the iron-sulfur cluster (ISC)<sup>2</sup> assembly machinery that is essential for biosynthesis of all cellular Fe/S proteins. The functional core of this system consists of the scaffold proteins Isu1p/Isu2p for the *de novo* synthesis of a transiently bound Fe/S cluster. In yeast, Fe/S cluster synthesis on Isu1p involves the cysteine desulfurase complex Nfs1p/Isd11p as the sulfur donor, Yfh1p (frataxin), and an electron transfer chain consisting of the ferredoxin Yah1p and its cognate reductase, Arh1p. The specialized Hsp70 chaperone Ssq1p, its cognate J-type co-chaperone Jac1p, the nucleotide exchange factor Mge1p, and the monothiol glutaredoxin Grx5p are involved in subsequent steps following Fe/S cluster synthesis on Isu1p. The ISC system has been inherited from bacteria that encode proteins of similar structure and function in the *isc* operon (3). In yeast, several of the ISC members are essential for cell viability underscoring the fundamental role of Fe/S protein maturation for the eukaryotic cell.

The mitochondrial ISC assembly system is also required for biosynthesis of cytosolic and nuclear Fe/S proteins (8–10). Their maturation further depends on the mitochondrial "ISC export machinery" that consists of the mitochondrial inner membrane ABC transporter Atm1p, the mitochondrial inter-membrane space sulfhydryl oxidase Erv1p, and glutathione (8, 11, 12). This export system is responsible for sequestering an unknown component from mitochondria to the cytosol to facilitate maturation of cytosolic and nuclear Fe/S proteins, a step carried out by the members of the cytosolic Fe/S protein assembly (CIA) system. The CIA machinery includes the cytosolic iron-only hydrogenase-like protein Nar1p, the soluble P-loop NTPases Cfd1p and Nbp35p, and the WD40 repeat protein Cia1p, which catalyze the maturation of cytosolic Fe/S proteins in an ordered pathway (13–16). All components are highly conserved in eukaryotes and essential for viability of *S. cerevisiae* (5, 7).

In *S. cerevisiae*, the disruption of the mitochondrial ISC assembly and export machineries induces the accumulation of iron within mitochondria (8) and the constitutive expression of a set of iron-regulated genes that are referred to as the iron regulon (17–19). Gene expression of the iron regulon is under control of the iron-responsive transcription factors Aft1p and

<sup>2</sup> The abbreviations used are: ISC, iron-sulfur cluster; CIA, cytosolic iron/sulfur protein assembly; WT, wild type; GFP, green fluorescent protein.

Aft2p (20–23). Under iron-limiting conditions, Aft1p shuttles from the cytosol into the nucleus where it acts as transcriptional activator (24). Because the impairment of mitochondrial Fe/S cluster formation is not associated with the depletion of cytosolic iron pools, it has been proposed that Aft1p requires a signal molecule produced and exported by the mitochondrial ISC machineries for proper sensing of iron (25, 26). Furthermore, defects in the ISC machinery are associated with heme deficiency (27–29). Biochemical analyses indicate that the inhibition of ferrochelatase, the last step of heme biosynthesis, by an unknown low molecular mass substance may be responsible for this inhibition (29).

To systematically understand the importance of Fe/S protein biogenesis for cellular homeostasis, we have carried out genome-wide comparative analyses of the transcriptional responses to defects in cellular Fe/S protein maturation in *S. cerevisiae*. In particular, we were interested in gaining insights into the regulatory cross-talks between cellular Fe/S protein maturation, respiration, heme biosynthesis, and the regulation of cellular iron homeostasis. We further sought to identify additional pathways affected by defects in cellular Fe/S protein maturation. We report on a dramatic remodeling of mitochondrial and cytosolic biochemical pathways as a result of defects in the mitochondrial ISC machineries. Most but not all of these processes are directly or indirectly connected to cellular iron and/or heme metabolism thus intimately linking the two major iron-dependent processes. In contrast, only mild transcriptional changes with no clear preference for any particular functional pathway were observed when the CIA machinery was compromised. These data indicate that the remodeling upon defects in the mitochondrial ISC machineries is not related to the biogenesis of a canonical cytosolic or nuclear Fe/S protein but rather to a signal emanating from mitochondria. Together, our data identify mitochondria in general and the mitochondrial ISC machineries in particular as a major regulatory device for multiple cellular processes, which show a tight connection to cellular iron and/or heme homeostasis.

## EXPERIMENTAL PROCEDURES

**Yeast Strains and Cell Growth**—Yeast strains used in this study are listed in supplemental Table SIV. Cells were cultivated in rich (YP), minimal (SC), “iron-poor” minimal medium lacking added iron chloride (30). Carbon sources were added at a concentration of 2% (w/v). Prior to microarray experiments, strains were cultivated in SC medium supplemented with 2% glucose (SD) for 40 h (WT, Gal-ATM1, Gal-NBP35) or 48 h (Gal-YAH1). To deplete Hem15p or Ssq1p to physiologically critical levels, Gal-HEM15 and Gal-SSQ1 cells were pre-cultivated for 3 days on SD plates.

**Microarray Analysis**—Strains were cultivated in parallel in SD medium supplemented with the minimal set of amino acids required for growth of the wild type strain (30). RNA was extracted from cells that were diluted from overnight cultures to an  $A_{600\text{ nm}}$  of 0.2 and cultivated in parallel to an  $A_{600\text{ nm}}$  of 0.5–0.6 using the RNeasy kit (Qiagen). An optional on-column DNase digestion was performed (Qiagen). RNA quality was analyzed by gel electrophoresis. RNA (12–15  $\mu\text{g}$ ) was transcribed into Cy3- or Cy5-labeled cDNA using the CyScribe

post-labeling kit (GE Healthcare) following the manufacturer’s protocol. Unincorporated nucleotides were removed by gel filtration using MicroSpin G-50 columns (GE Healthcare). Efficiency of cDNA synthesis and Cy-Dye incorporation were monitored by measuring the absorption at 260 nm (cDNA), 550 nm (Cy3), and 650 nm (Cy5). For each Gal mutant, microarray experiments were performed twice with RNA isolated from independent cultures grown on different days. Cell viability at the point of RNA extraction was analyzed by incubation of serial dilutions on SD minimal plates and was found not to be compromised.

Yeast microarrays (Y6.4k6; University Health Network Microarray Centre, Toronto, Canada) were pre-hybridized for 2 h at 37 °C in 5 $\times$  SSC buffer containing 0.1% SDS and 1% bovine serum albumin and rinsed twice with water and once in isopropyl alcohol. Labeled probes were concentrated to a final volume of  $\sim 3\ \mu\text{l}$ , pooled, added to 54  $\mu\text{l}$  of DIG Easy Hyb solution buffer (Roche Applied Science) supplemented with 3  $\mu\text{l}$  of yeast tRNA (10 mg/ml) and 3  $\mu\text{l}$  of denatured salmon sperm DNA (10 mg/ml), and incubated at 62 °C for 5 min. Hybridizations were carried out for 18 h at 37 °C in a hybridization chamber (Corning Glass). Hybridized arrays were removed from the coverslip by immersing in 1 $\times$  SSC buffer. Slides were washed three times with 1 $\times$  SSC, 0.2% SDS buffer for 15 min at 50 °C in a hybridization oven with agitation. Arrays were rinsed at room temperature in 1 $\times$  SSC buffer, 4–5 times in 0.1 $\times$  SSC buffer, and dried by spinning in 50-ml Falcon tubes for 5 min by 1500 rpm. A detailed protocol for hybridization can be obtained from the University Health Network website.

Fluorescence intensities were captured by using the scanner ScanArray Express (PerkinElmer Life Sciences). Spot intensities were extracted from a scanned image with ImaGene 3.0 (BioDiscovery, Inc.). To account for spot differences, the background-corrected ratio of the two channels were calculated, and log<sub>2</sub> was transformed. To standardize the raw data we used a spatial- and intensity-dependent standardization (the lowest scatter plot) to correct for inherent bias on each chip (similar to Ref. 31). As each gene was spotted twice on the array, mean log ratios were calculated for each slide and also for replicate slides. Differentially expressed genes were selected by the fold change.

**Northern Blot Analysis**—20  $\mu\text{g}$  of total RNA was separated on a denaturing agarose gel and blotted to nylon membrane (32). <sup>32</sup>P-Labeled DNA probes were generated by random priming of DNA fragments containing the entire open reading frames of *HEM15*, *HMX1*, and *ACT1*, respectively. Hybridization was carried out in ULTRAhyb buffer (Ambion).

**Promoter Assays**—The promoter strength of the *FET3* promoter was determined as described previously (26), and the promoter strength of the *CYC1* promoter was determined using vector pCYC1-GFP, which harbors region –1 to –900 bp upstream of the *CYC1* open reading frame in front of the GFP gene of vector pHK12, a *URA3* derivative of pPS1372 (33). Promoter analyses based on luciferase were carried out with vector p416MET-hRluc that harbored the *Renilla reniformis hRluc* gene from vector pGL4.70 (Promega) between the HindIII and Sall sites. The upstream regions of *BIO2* (1 kb), *ERG3* (1 kb), *GLT1* (700 bp), and *YHB1* (1 kb) were inserted into SacI and HindIII restriction sites replacing the *MET25* promoter. Cells



## Response to Fe/S Protein Maturation Defects in Yeast

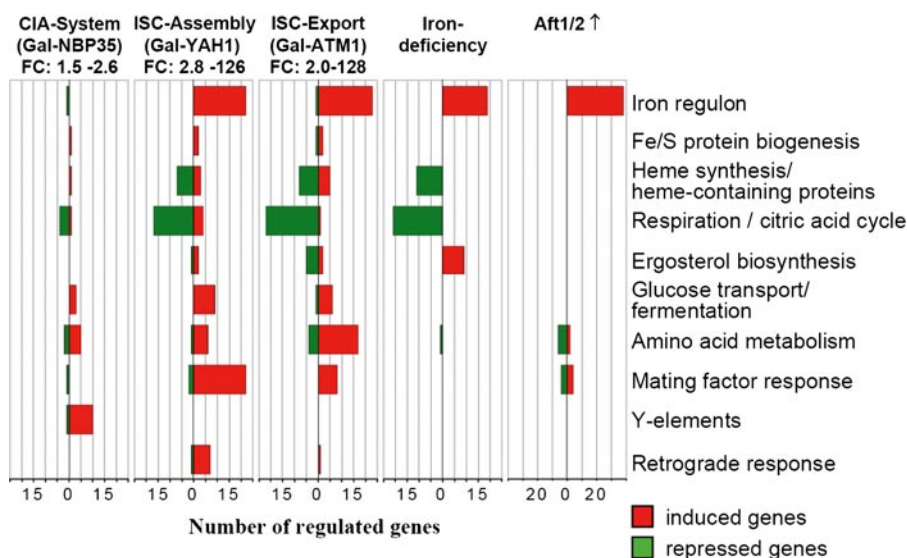


**FIGURE 1. Overview of the transcriptional responses of *S. cerevisiae* to depletion of Yah1p, Atm1p, and Nbp35p.** Genes affected upon depletion of the glucose-repressible Gal-ATM1, Gal-YAH1, and Gal-NBP35 cells were identified by DNA microarray analyses (see Table 1 and supplemental Tables SI and SII) and assigned to the indicated functional categories. Numbers indicate the sum of regulated genes in each category. Experiments were performed in duplicate with RNA isolated from independent cultures grown on different days. (FC, fold change of the transcriptional response.) Data for the transcriptional response to iron deprivation was taken from Ref. 49 and that of cells overproducing Aft1p or Aft2p were from Ref. 21. (Cut off, >2.0-fold induced; >1.7-fold repressed.)

were grown in SD medium and diluted to  $A_{600\text{ nm}} = 0.2$ , and promoter analyses were carried out with cells grown to mid-log phase. For iron starvation, the medium was supplemented with 50  $\mu\text{M}$  bathophenanthroline. For the analysis of GFP expression, cells were collected by centrifugation and resuspended to  $A_{600\text{ nm}} = 1$  in water, and the fluorescence emission at 513 nm was recorded. The excitation wavelength was 485 nm. For luciferase assays, cells were diluted to  $A_{600\text{ nm}} = 0.1$  in water; fractions (5–10  $\mu\text{l}$ ) were diluted in 100  $\mu\text{l}$  of water supplemented with 2  $\mu\text{l}$  of a 1:500 dilution of ViviRen substrate (Promega), and the cellular luminescence was recorded in a scintillation counter. The background signal obtained with cells lacking the respective reporter was subtracted. Values are averages of duplicate measurements of at least four independent cultures.

**Miscellaneous Methods**—For determination of the cellular heme content, cells were grown for 16 h in iron-free SD medium supplemented with 10  $\mu\text{Ci}$  of  $^{55}\text{FeCl}_3$  and 1 mM ascorbate at 30  $^\circ\text{C}$ . Subsequently, radiolabeled  $^{55}\text{Fe}$ -heme was extracted by *n*-butyl acetate and quantified by liquid scintillation counting as described previously (34). The following published methods were used: manipulation of DNA and PCR (32); transformation of yeast cells (35); isolation of yeast mitochondria and post-mitochondrial supernatant (36); immunostaining (37); and determination of enzyme activities and iron contents (8), ferrochelatase (38), and catalase (39). Error bars represent the standard deviation.

## RESULTS

To analyze the global consequences of defects in cellular Fe/S protein maturation in *S. cerevisiae*, we carried out DNA microarray analyses with regulatable yeast mutants that carry the respective gene representatives of each of the three biosynthetic systems under the control of the galactose-inducible, glu-

cose-repressible *GAL1–10* promoter. In particular, we used the mitochondrial ISC assembly mutant Gal-YAH1 (40), the ISC export mutant Gal-ATM1 (8), and the CIA mutant Gal-NBP35 (15). To define the set of genes that were responsive to depletion of Yah1p, Atm1p, or Nbp35p, wild type and the corresponding mutants were cultivated in parallel in minimal medium supplemented with glucose and a minimal set of amino acids. RNA was isolated, and genes showing an altered expression level with respect to the wild type control cells were identified by DNA microarray analyses.

**Weak Transcriptional Response upon Depletion of Nbp35p**—The transcriptional response of cells depleted of the CIA member Nbp35p was rather weak with a maximum change of only 2.6-fold. A total number of 117 genes were identified that displayed at least a

1.5-fold transcriptional change in comparison with wild type cells (Fig. 1, Table 1, and supplemental Table SI). Preliminary microarray analyses of cells depleted of two other CIA members, Nar1p and Cia1p, gave similar results (data not shown). The transcriptional response showed hardly any overlap with cells depleted of Yah1p or Atm1p (see below). The most prominent sets of genes induced upon depletion of Nbp35p were members of the so called Y' elements (Table 1). These are sub-telomerically encoded genes, some of which encode proteins with potential helicase activity (41). These components are suggested to play a role in telomerase-independent telomere maintenance. These telomerase-responsive genes are induced upon nitrogen depletion, in stationary phase, and in aging cells (42). Their induction in Gal-NBP35 and also Gal-YAH1 cells may thus reflect a response to the depletion of an essential gene in *S. cerevisiae*. In addition, the expression profile of Nbp35-depleted cells included several genes that are known to be regulated in response to mitochondrial dysfunction. Several genes of mitochondrial ribosomal proteins and of the  $F_1F_0$ -ATP synthase were slightly repressed. A similar repression is observed during a diauxic shift (43). In parallel, hexose transporters were induced to some extent. Furthermore, the *CIT2* gene encoding the peroxisomal citrate synthase was weakly induced. This may indicate an induction of the so-called retrograde response, which is activated upon mitochondrial perturbations (44, 45). However, the response was rather weak, and its reason is unclear, because the depletion of Nbp35p does not significantly affect mitochondrial function (15).

Remarkably, the transcriptional profile of Nbp35-depleted cells did not show any significant compensatory response to the biochemical defects in cytosolic and nuclear Fe/S protein maturation. *ISU2* was the only gene encoding an Fe/S assembly factor, which showed a slightly enhanced expression. *SUL1* encoding the sulfate permease of the plasma membrane was

TABLE 1

Selected genes modulated upon depletion of the mitochondrial ISC assembly component *Yah1p*, the ISC export component *Atm1p*, and the CIA member *Nbp35p*

Fold changes are given in relation to those of the wild type cultivated under the same experimental conditions. Values are averages of two biological and technical experiments, including dye swaps between experiment and reference sample. Repressed genes are indicated by -. (See supplemental tables for complete lists.)

Open reading frame	Gene	Description	Average fold change		
			Gal-YAH1	Gal-ATM1	Gal-NBP35
<b>Iron regulon (Aft1p/Aft2p)/iron-responsive proteins</b>					
YHL040C	<i>ARN1</i>	Siderophore transporter	33.7 ± 6.1	16.5 ± 1.4	-1.1 ± 0.2
YMR058W	<i>FET3</i>	Cell surface ferroxidase	34.5 ± 14	14.1 ± 1.1	-1.6 ± 0.5
YDR534C	<i>FIT1</i>	Retention of siderophore iron	162 ± 15	111 ± 25	1.4 ± 0.3
YLR214W	<i>FRE1</i>	Ferric (and cupric) reductase	5.1 ± 0.4	5.8 ± 0.4	1.03 ± 0.15
YER145C	<i>FTR1</i>	Iron permease	15.8 ± 3.5	9.8 ± 0.2	-1.2 ± 0.15
<b>Fe/S protein biogenesis</b>					
YPL059W	<i>GRX5</i>	Glutaredoxin	-2.8 ± 0.5	-2.2 ± 0.2	-1.15 ± 0.2
YPL135W	<i>ISU1</i>	Scaffold protein	4.0 ± 0.8	3.2 ± 0.7	1.3 ± 0.1
YOR226C	<i>ISU2</i>	Scaffold protein	4.0 ± 2.0	2.1 ± 0.5	1.5 ± 0.2
<b>Heme metabolism and heme-dependent proteins</b>					
YOR176W	<i>HEM15</i>	Ferrochelatase (protoheme ferrolyase)	-5.4 ± 1.2	-3.1 ± 0.4	-1.1 ± 0.15
YLR205C	<i>HMX1</i>	Heme oxygenase	9 ± 1.2	7.2 ± 0.5	1.45 ± 0.1
YGR088W	<i>CTT1</i>	Catalase T (cytosolic)	-4.5 ± 1.5	-1.85 ± 0.15	-1.13 ± 0.2
YLR256W	<i>HAP1</i>	Heme-responsive transcription factor	4.5 ± 1	1.9 ± 0.5	1.05 ± 0.15
YGR234W	<i>YHB1</i>	Flavo-hemoglobin	-11 ± 2.8	-10.5 ± 0.5	1.2 ± 0.1
<b>Respiration and citric acid cycle</b>					
YJR048W	<i>CYC1</i>	Cytochrome- <i>c</i> isoform 1	-11.7 ± 2.4	-8.7 ± 1.3	-1.1 ± 0.2
YGL187C	<i>COX4</i>	Cytochrome <i>c</i> oxidase subunit IV	-3.6 ± 0.4	-2.3 ± 0.7	-1.2 ± 0.2
YEL024W	<i>RIP1</i>	Complex III/Rieske Fe/S protein	-6.3 ± 1.1	-4.8 ± 1.4	-1.1 ± 0.1
YKL148C	<i>SDH1</i>	Complex II flavoprotein subunit	-5.1 ± 0.4	-3.3 ± 0.3	-1.4 ± 0.2
YNL037C	<i>IDH1</i>	Isocitrate dehydrogenase	9.9 ± 1.2	2.1 ± 0.3	1.1 ± 0.15
YLR304C	<i>ACO1</i>	Aconitase	1.2 ± 0.1	-2.6 ± 0.2	-1.3 ± 0.3
<b>Ergosterol biosynthesis</b>					
YNL111C	<i>CYB5</i>	Cytochrome <i>b</i> <sub>5</sub>	-3.5 ± 0.2	-2.8 ± 1.0	-1.2 ± 0.1
YLR056W	<i>ERG3</i>	C-5 sterol desaturase	6.8 ± 0.3	3.2 ± 0.5	1.4 ± 0.1
YER044C	<i>ERG28</i>	Endoplasmic reticulum membrane protein	-2.1 ± 0.3	-2.7 ± 0.5	-1.4 ± 0.2
YHR042W	<i>NCP1</i>	NADP-cytochrome P450 reductase	3.5 ± 0.5	2.5 ± 0.8	1.1 ± 0.1
<b>Glucose transport and fermentation</b>					
YHR094C	<i>HXT1</i>	Hexose permease	3.2 ± 0.8	2.0 ± 0.2	1.5 ± 0.2
YHR096C	<i>HXT5</i>	Hexose permease	5.4 ± 0.8	1.8 ± 0.2	1.7 ± 0.3
YOR374W	<i>ALD4</i>	Mitochondrial aldehyde dehydrogenase	3.7 ± 0.8	1.9 ± 0.2	1.5 ± 0.3
<b>Amino acid metabolism</b>					
YFL055W	<i>AGP3</i>	General amino acid permease	2.8 ± 0.1	1.1 ± 0.2	1.5 ± 0.2
YDR019C	<i>GCV1</i>	Glycine decarboxylase T subunit	1.2 ± 0.3	2.8 ± 0.1	-1.1 ± 0.1
YDL171C	<i>GLT1</i>	Glutamate synthase	-1.8 ± 0.2	-1.3 ± 0.2	-1.2 ± 0.1
YGL009C	<i>LEU1</i>	3-Isopropylmalate isomerase	-11.3 ± 1.5	-10.9 ± 0.2	1.4 ± 0.5
YNL268W	<i>LYP1</i>	Lysine permease	2.9 ± 0.3	2.4 ± 0.3	1.6 ± 0.2
<b>Biotin metabolism</b>					
YGR286C	<i>BIO2</i>	Biotin synthase	-2.0 ± 0.1	-1.9 ± 0.2	-1.5 ± 0.1
YNR056C	<i>BIO5</i>	Biotin synthesis	4.4 ± 0.8	3.0 ± 0.2	-1.0 ± 0.3
YGR065C	<i>VHT1</i>	Biotin transporter	2.6 ± 0.3	4.8 ± 0.2	-1.3 ± 0.2
<b>Mating factor response</b>					
YNL145W	<i>MFA2</i>	A-factor precursor	-21.5 ± 3.7	1.0 ± 0.1	-1.3 ± 0.2
YPL156C	<i>PRM4</i>	Pheromone-Regulated protein	3.3 ± 0.7	1.4 ± 0.2	-1.1 ± 0.1
YPL187W		Mating factor $\alpha$	38 ± 6	-1.3 ± 0.2	1.1 ± 0.1
YJR026W		Transposable element gene	7.5 ± 3	2.2 ± 0.4	1.6 ± 0.3
<b>Y-elements</b>					
YHL050C		Similar to other subtelomerically encoded proteins	2.6 ± 0.4	2.0 ± 0.4	2.0 ± 0.3
YLR466W	<i>YRF1</i>	Y' helicase (subtelomerically encoded)	3.3 ± 0.5	1.8 ± 0.4	1.8 ± 0.1
YPR204W		Similar to other subtelomerically encoded proteins	2.9 ± 0.3	1.6 ± 0.1	2.1 ± 0.5
<b>Retrograde response</b>					
YCR005C	<i>CIT2</i>	Peroxisomal citrate synthase	2.9 ± 0.4	-1.4 ± 0.2	1.9 ± 0.2
YPL265W	<i>DIP5</i>	Glutamate/aspartate permease	6.6 ± 1.3	1.1 ± 0.2	1.9 ± 0.4
YOR136W	<i>IDH2</i>	Isocitrate dehydrogenase	4.7 ± 0.5	1.1 ± 0.2	1.1 ± 0.1
YOR222W	<i>ODC2</i>	Mitochondrial 2-oxoglutarate transporter	-4.7 ± 1.1	-1.4 ± 0.3	-1.4 ± 0.2

induced, most likely in response to a sulfur assimilation deficiency of the *NBP35* mutant caused by the loss of function of sulfite reductase, a cytosolic Fe/S protein (supplemental Table S1). In addition, a weak induction of the *BAP2/3* genes was observed. These encode permeases for branched chain amino acids, and their induction may reflect a leucine deficiency because of loss of the activity of the Fe/S protein Leu1p in *Nbp35p*-depleted cells. In conclusion, only slight changes with no obvious preference for a specific pathway or functional cat-

egory were detectable upon repression of *NBP35*. It appears that this gene, and possibly other CIA components, is not a major trigger to alter gene expression in yeast. This observation was surprising as *NBP35* is essential for viability of *S. cerevisiae* (15).

*Multiple Pathways Linked to Iron Metabolism Are Re-modeled upon Depletion of Atm1p and Yah1p*—Strong transcriptional responses were observed upon depletion of *Atm1p* and *Yah1p*, contrasting the findings with *Nbp35p*. In both cases

## Response to Fe/S Protein Maturation Defects in Yeast

more than 200 genes displayed a 2-fold or larger transcriptional change in comparison with wild type cells, with a maximum induction of ~120-fold (Fig. 1, Table 1, and supplemental Table SII). The transcriptional profiles of both mutants displayed a remarkably high degree of overlap. A large number of genes of the Aft1p/Aft2p-dependent iron regulon (referring to the results of Ref. 21) were significantly induced in both mutants. In addition, several other iron-responsive genes encoding proteins involved in iron uptake and transport were induced that are not canonical Aft1p or Aft2p targets, such as *FET4* or *FTH1* (21). Most likely, these genes are also under the control of the Aft transcription factors but respond more weakly. These results are consistent with earlier findings that indicate that the constitutive activation of the Aft transcription factors is one of the general consequences of impaired ISC machineries (see e.g. Refs. 8, 18, 25, 26, 46).

The second major response to depletion of *Atm1p* and *Yah1p* was a massive repression of genes encoding proteins of the mitochondrial respiratory chain (Fig. 1 and Table 1). This set includes genes for several subunits of the respiratory complexes II–IV, the  $F_1F_0$ -ATP synthase, and the two cytochrome *c* isoforms. In fact, most of the genes that were repressed in both mutants belong to this category. In case of *Yah1p* depletion, this expression pattern may in part reflect a direct response to the respiratory deficiency resulting from an impaired mitochondrial Fe/S protein biogenesis. This conclusion is substantiated by the modulation of several genes (such as *CIT2* and *ODC2*) that belong to the retrograde response, a physiological response that is triggered upon mitochondrial dysfunction (44, 45, 47). However, these latter genes are virtually unaffected upon depletion of *Atm1p* despite the strong overlap in respiratory genes (supplemental Table SII). This indicates that additional reasons may underlie these responses.

In yeast, genes of the respiratory chain are regulated by iron availability and are repressed upon iron limitation (48, 49). Remarkably, all major functional categories that are transcriptionally modulated in response to iron starvation in yeast are also altered in ISC mutants (Fig. 1). This strongly suggests that the transcriptional repression of respiratory chain complexes in cells with defective ISC machineries can be explained by the deregulated iron homeostasis in these cells. As a complementary effect to the repression of respiratory components, genes involved in sugar acquisition and utilization were strongly induced in both the *YAH1* and *ATM1* mutants despite the fact that these cells were grown under fermentative conditions (Fig. 1 and Table 1). Apparently, the lack of functional Fe/S proteins imposes an even stronger induction of fermentative genes. The transcriptional changes of several genes for key enzymes of the tricarboxylic acid cycle most likely belong to the same responsive circuit (Fig. 2).

Depletion of *Atm1p* and *Yah1p* affected the gene expression pattern of several other biosynthetic pathways, including the biosynthesis of ergosterol, biotin, and the metabolism of several amino acids (Figs. 1 and 2, Table 1, and supplemental Table SII). Because several genes of the ergosterol biosynthetic pathway are regulated by iron availability in yeast, their changed expression pattern in the *ATM1* and *YAH1* mutants may be the indirect response to a deregulated cellular iron homeostasis. In

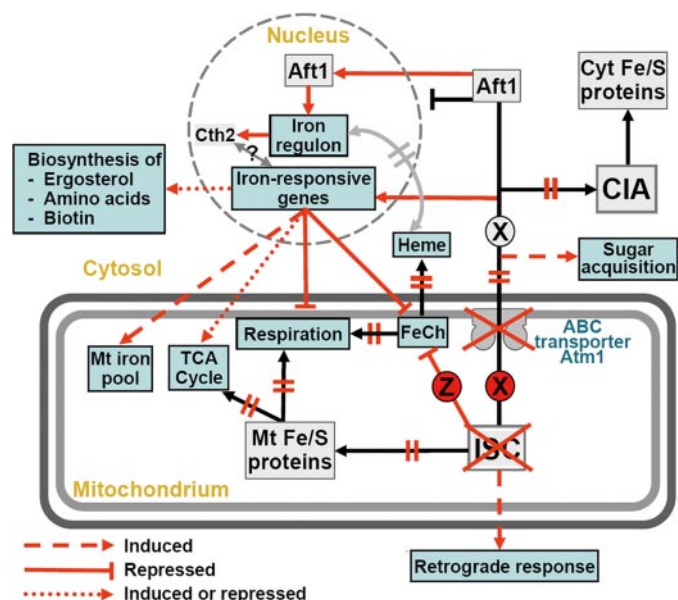


**FIGURE 2. Model for the crucial role of mitochondria as major regulators of numerous processes connected to cellular iron and heme homeostasis.** Under normal physiological conditions (black arrows), the mitochondrial (Mt) Fe/S cluster assembly system (ISC) produces a signal molecule (X) that is exported to the cytosol by the ABC transporter *Atm1p*. Compound X is required for both the formation of cytosolic Fe/S proteins and the retention of the Aft1p (and Aft2p) transcription factor(s) in the cytosol. Upon defects in the mitochondrial ISC or ISC export (*Atm1p*) systems (red lines), low cytosolic levels of this regulatory molecule result in defects of cytosolic Fe/S protein assembly (CIA) and a substantial transcriptional remodeling. A major effect is the constitutive induction of the iron regulon by the transcription factor(s) Aft1p (and Aft2p), which will increase cellular iron acquisition (21). A second important physiological alteration is the remodeling of numerous iron-responsive processes. This includes the repression of mitochondrial respiration and heme synthesis, which serves to balance the utilization of iron by the main cellular iron consumers, namely Fe/S protein and heme biosynthesis. In addition, Cth2p, a member of the iron regulon, contributes to the repression of genes involved in respiration and other iron-responsive pathways under iron-depletion conditions (49). The magnitude and the precise mechanism of the contribution of Cth2p, however, are unresolved. Respiratory deficiency in ISC-compromised cells is compensated by induction of genes involved in sugar acquisition. The heme deficiency observed upon defects in the ISC assembly system is caused by transcriptional repression of ferredoxin (FeCh) and the accumulation of a regulatory molecule (Z) that inhibits the activity of this enzyme catalyzing the last step of heme biosynthesis (29). The levels of heme, however, do not contribute to the regulation of (most) genes of the iron regulon and vice versa (gray line). Further transcriptional changes affect iron-responsive genes of the mitochondrial tricarboxylic acid (TCA) cycle and the pathways of ergosterol, amino acid, and biotin synthesis.

addition, low levels of heme may contribute to the altered expression of genes involved in ergosterol biosynthesis, because this pathway involves heme-containing enzymes (50). The biosynthetic pathway for biotin displays an iron-dependent expression profile (48). The genes affected upon depletion of *Atm1p* and *Yah1p* (*VHT1* and *BIO5*) encode plasma membrane transporters for biotin and its precursors and are regulated by Aft1p (21), indicating that a deregulated iron homeostasis is responsible for the transcriptional changes of genes involved in biotin synthesis in these strains.

Both the *YAH1* and *ATM1* mutants showed strong transcriptional changes of genes encoding heme-containing proteins (Table 1 and supplemental Table SII). This effect was generally stronger in the *YAH1* mutant consistent with its direct function in the synthesis of heme (51). Besides several genes of respiratory chain components, genes for the cytosolic catalase



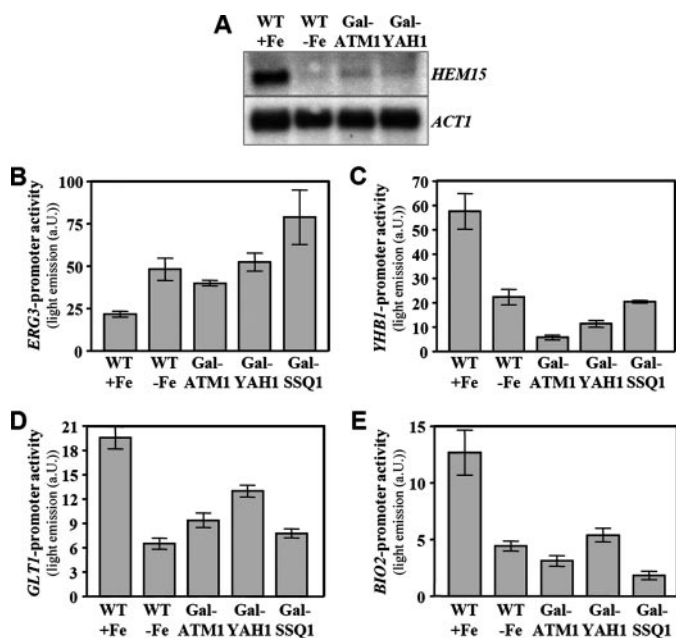


**FIGURE 3. Depletion of the mitochondrial ISC systems affects the expression of iron-regulated genes.** *A*, Northern blot analysis of *HEM15* transcription. Total RNA was isolated from exponentially growing WT cells, wild type cells cultivated overnight in the presence of 50  $\mu$ M bathophenanthroline (*WT-Fe*), and depleted Gal-ATM1 or Gal-YAH1 cells. Equal amounts of RNA were separated on agarose gels, blotted onto nylon membranes, and hybridized with  $^{32}$ P-labeled probes for *HEM15* and *ACT1*. *B-E*, wild type and the regulatable strains Gal-ATM1, Gal-YAH1, and Gal-SSQ1 were transformed with the reporter plasmids p416*ERG3*-hRluc (*B*), p416*YHB1*-hRluc (*C*), p416*GLT1*-hRluc (*D*), or p416*BIO2*-hRluc (*E*). Strains were grown in minimal medium supplemented with glucose (SD) to repress *ATM1*, *YAH1*, and *SSQ1* in the corresponding Gal strains. Promoter activities were determined by measuring the luminescence of intact cells grown to mid-log phase. Error bars indicate the standard deviation of the measurements after 48 and 72 h of depletion (*Gal-ATM1* and *Gal-YAH1*) and 86 h (*Gal-SSQ1*). Wild type cells cultivated in SD (*WT+Fe*) or SD medium containing 50  $\mu$ M bathophenanthroline (*WT-Fe*) were analyzed in parallel. Error bars indicate the standard deviation ( $n \geq 8$ ).

(*CTT1*), the yeast flavohemoglobin (*YHB1*), and cytochrome *b*<sub>2</sub> (*CYB2*) of the mitochondrial intermembrane space were repressed, whereas *NCPI* encoding a cytochrome P450 reductase involved in ergosterol biosynthesis and *HAPI* encoding the heme-dependent transcription factor Hap1p were induced. Of the genes involved in heme biosynthesis, ferrochelatase (*HEM15*) was repressed, whereas *HMX1*, a putative heme oxygenase, was strongly induced. Remarkably, genes for the biosynthesis of porphyrins, including the key pacemaker enzyme, 5-aminolevulinic synthase (*HEM1*), were unaffected, with the exception of *HEM13* which was 2-fold repressed in Gal-YAH1 cells. In accordance with the microarray data, *HEM15* mRNA levels were ~10-fold reduced in depleted Gal-ISC cells, and the corresponding transcript was almost undetectable in iron-starved wild type cells, confirming that *HEM15* is repressed upon iron deprivation (Fig. 3*A*) (48). These observations indicate a general remodeling of the biosynthesis and cellular distribution of heme, but not of porphyrins, in response to defects in the mitochondrial ISC assembly and export systems. These effects will be further analyzed below.

*ISU1* and *ISU2* were the only genes encoding components involved in cellular Fe/S protein maturation that were significantly induced in both the *YAH1* and *ATM1* mutant (Table 1).

Because the *ATM1* mutant displays no obvious defects in mitochondrial Fe/S protein maturation, this response is likely triggered by the loss of function of cytosolic Fe/S proteins. *LEU1* was the only gene encoding an Fe/S protein that was significantly repressed in the *YAH1* and *ATM1* mutants. The repression of *RIP1* encoding the Rieske Fe/S protein, respectively, is partially explained as a consequence of the impairment of respiration. Apparently, defects in cellular Fe/S protein biogenesis do not trigger a massive compensatory transcriptional response of genes encoding Fe/S proteins and Fe/S protein assembly factors in *S. cerevisiae*, despite the fact that Fe/S cluster assembly is an essential process in yeast.

Genes for components involved in the metabolism of amino acids were induced to a greater extent in the *ATM1* mutant (supplemental Table SII). These include several genes involved in branched-chain amino acid biosynthesis, such as the *BAT*, *BAP*, and *LEU* genes, which may be regulated in response to the loss of function of the Fe/S proteins Ilv3p and/or Leu1p. *BAP2/3* were also weakly induced in cells depleted of Nbp35p that show low Leu1p activities. The connection between the depletion of Atm1p and the metabolism of lysine, arginine, and glycine, however, is not obvious at first glance. The changes in the transcriptional profiles of these pathways may be triggered by a general amino acid deficiency that may result from low activities of Fe/S proteins involved in amino acid biosynthesis. For example, low activities of the glutamate synthase Glt1p, an iron-regulated Fe/S protein, result in defects in ammonia assimilation (48). In both Gal-ATM1 and Gal-YAH1 cells, the activation of the response to nitrogen deprivation is indicated by the induction of the master regulator of the general control of nitrogen, Gcn4p (52). Similar to findings for depletion of Nbp35p, genes involved in sulfur assimilation were modulated in the *YAH1* and *ATM1* mutants, most likely in response to the loss of function of sulfite reductase (*ECM17/MET10*).

Genes that are summarized in Fig. 1 under mating factor response were most strongly induced in the *YAH1* mutant. This functional category includes genes encoding mobile elements that are strongly induced in the presence of mating factors. Most likely this response is caused by the depletion of a crucial gene, which may trigger a mating response as a last resort for a dying cell to survive, similar to the induction of Y-elements seen in the *NBP35* mutant. Finally, the transcriptional profiles of both strains include various differentially regulated genes with so far unknown function.

Taken together, the microarray analysis indicates a central role of the mitochondrial ISC assembly and export systems in the regulation of numerous cellular processes, most of which are connected to iron or heme metabolism (Fig. 2). Clearly, the transcriptional profiles of cells with defective ISC assembly and export machineries display a strikingly large overlap with the transcriptional response of yeast cells to iron deprivation (48, 49) (Fig. 1). The induction of the iron-deprivation response is likely the decisive factor underlying the transcriptional response to mitochondrial ISC assembly and export defects. This response encompasses a considerably larger number of genes than that observed upon the constitutive activation of the Aft transcription factors that is confined mainly to the induc-

tion of the iron regulon (Fig. 1) (21). Thus, the induction of the iron regulon, a well known characteristic of cells with impaired ISC assembly and export machineries, is just one of the consequences of the apparent iron-deprivation status prevailing in these cells. The overlap with the response to iron starvation, however, is not complete, as the transcription profiles of ISC mutants contain additional genes that are not iron-responsive, such as those belonging to the retrograde response or the metabolism of lysine, glycine, and arginine. In addition, the alterations in central mitochondrial pathways, such as respiration, heme synthesis, and the tricarboxylic acid cycle also likely reflect a response to loss of function of mitochondrial Fe/S proteins.

Mitochondrial control over cellular iron metabolism is mediated by a regulatory signal that appears to be produced and exported by the ISC assembly and export machineries, but it is not related to a canonical extramitochondrial Fe/S protein. Low cytosolic levels of this regulatory molecule result in both defects of cytosolic Fe/S protein maturation and a substantial transcriptional remodeling of the cellular iron and heme metabolism. In conclusion, the activities of the ISC machineries serve as an important physiological sensor of the mitochondrial iron status, and, by signaling to the cytosol, contribute to maintain the balance between intracellular iron demands and cellular iron supply (Fig. 2).

*Depletion of ISC Components Affects Transcription of Both AFT-dependent and -independent Iron-responsive Genes*—The microarray analysis indicated that a large number of Aft1/2p-independent iron-responsive genes also respond to ISC defects. These include most genes involved in respiration and the metabolism of ergosterol, biotin, and heme (Fig. 1 and supplemental Table SII) (48, 49). To specifically address whether their transcriptional remodeling in ISC mutants is indeed mediated by the apparent iron-deprivation status prevailing in these cells, we studied the expression of the iron-regulated genes *BIO2*, *ERG3* (encoding the C-5 sterol desaturase), *GLT1* (encoding the Fe/S protein glutamate synthase), and *YHB1* (encoding mitochondrial flavohemoglobin). These genes are not induced in cells overproducing Aft1p or Aft2p cells (21, 53) (Fig. 1). Reporter plasmids that harbor 1-kb upstream regions of these genes in front of the *Renilla* luciferase gene were transformed into wild type, Gal-ATM1, Gal-YAH1, and Gal-SSQ1 cells. Cells were cultivated under repressive conditions, and promoter strengths were determined by recording the luciferase-specific luminescence. In case of the *ERG3* gene, the promoter activity increased 1.8–3.6-fold in cells depleted of Atm1p, Yah1p, and Ssq1p compared with wild type cells (Fig. 3B). A similar 2.2-fold induction was observed in wild type cells grown under iron-limiting conditions. Thus, the induction of *ERG3* in cells depleted of ISC components was indeed similar to that of an iron-starved cell. Comparable results were obtained for the other three iron-regulated genes that are repressed (Fig. 3, C–E). The findings of the transcriptional analyses for *ERG3*, *YHB1*, and that of the Northern blot analysis of *HEM15* (Fig. 3A) are in qualitative agreement with those of our microarray data (Table 1). The extent of repression of *BIO2* and *GLT1* was slightly below the set of thresholds for the microarray analyses (Table 1). Thus, the transcription profiles of these representa-

tive iron-responsive genes support the general conclusion that cells with defects in the mitochondrial ISC assembly and ISC export apparatus show the full transcriptional response of yeast to iron limitation (Fig. 2).

*Repression of Respiratory Genes in Atm1p- and Yah1p-depleted Cells Results from a Combination of Several Different Causes*—Although the constitutive induction of the iron regulon in Atm1p- and Yah1p-depleted cells is likely mediated by activation of Aft1p/Aft2p (26), the reason for the repression of genes involved in mitochondrial respiration in these cells is less clear. Repression may be induced by respiratory deficiency caused by Fe/S protein defects, the heme deficiency prevalent in ISC-depleted cells (29), a limitation of physiologically available iron in mitochondria (39), or a combination of these. To dissect these effects, we analyzed the transcriptional activity of the promoter of *CYC1* that was significantly repressed in Gal-ATM1 and Gal-YAH1 cells (Table 1). A reporter plasmid, pCYC1-GFP, was constructed that harbors the 1-kb upstream region of *CYC1* in front of the GFP open reading frame. Gal-ATM1, Gal-YAH1, and Gal-SSQ1 cells carrying this reporter plasmid were cultivated in SD medium, and the promoter strength of *CYC1* was determined by recording the GFP-specific fluorescence emission. The transcriptional activity of the *CYC1* promoter decreased 3-fold in cells depleted of Yah1p and Atm1p and 4-fold in Gal-SSQ1 cells compared with wild type cells (Fig. 4A). Apparently, the repression of respiratory genes is a general characteristic of all ISC mutants. Likewise, in the respiration-deficient strains *aco1Δ* (aconitase), *cyt2Δ* (cytochrome  $c_1$  heme lyase), *sod1Δ* (Cu/Zn superoxide dismutase), and Gal-Hem15 (ferrochelatase), the *CYC1* promoter strength was reduced by a similar margin (2.2–2.6-fold) (Fig. 4B). Because all these respiration-deficient mutants carried primary defects in different pathways (tricarboxylic acid cycle deficiency in *aco1Δ*, loss of respiratory complex III in *cyt2Δ*, oxidative stress in *sod1Δ*, heme deficiency (Gal-HEM15), or loss of mitochondrial Fe/S protein activity), multiple biochemical reasons, including defects in Fe/S protein biogenesis, induce the transcriptional repression of genes involved in respiration.

Upon iron deprivation, the promoter strength of *CYC1* was 6-fold lower than under iron-replete conditions in our W303 strain background, confirming that respiratory genes are repressed under iron-limiting conditions in yeast (Fig. 4C) (49). Mitochondria isolated from iron-starved yeast cells contained substantially lower activities of aconitase, the respiratory complexes II (succinate dehydrogenase) and IV (cytochrome oxidase), and ferrochelatase compared with those of mitochondria from iron-replete cells, whereas the activity of malate dehydrogenase as a control enzyme was hardly changed (Fig. 4D). In parallel, the activity of alcohol dehydrogenase was significantly increased in iron-starved yeast cells (not shown). Thus, iron deprivation induces a similar respiratory incompetence as defects in Fe/S protein maturation or heme deficiency.

This observation raised the question to what extent the regulatory mechanisms that underlie the repression of respiratory genes in cells defective in Fe/S protein biogenesis and under iron limitation were transmitted through the Aft1p-dependent iron regulon. We therefore determined the promoter strength



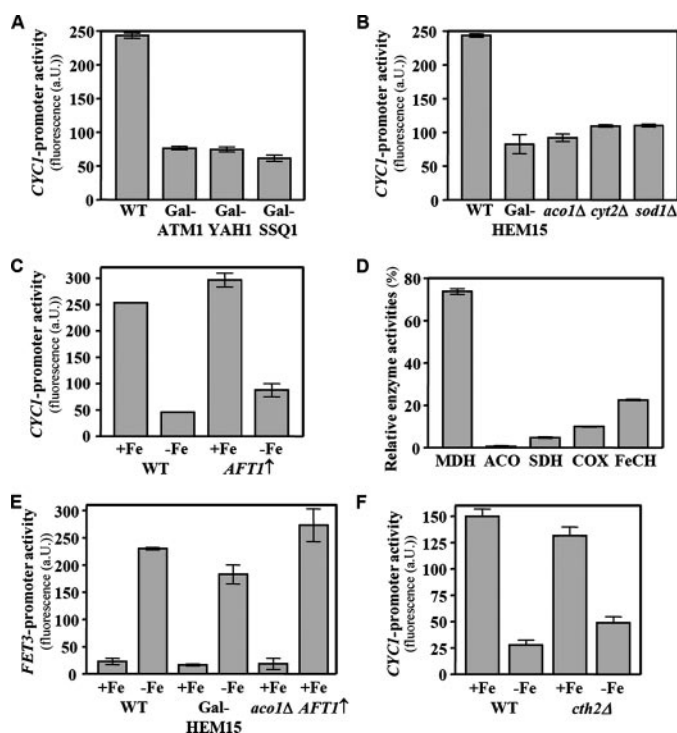


**FIGURE 4. The status of mitochondrial ISC systems affects the expression of respiratory genes.** WT yeast cells and the regulatable strains Gal-ATM1, Gal-YAH1, and Gal-SSQ1 (A), Gal-HEM15 (B), or the deletion strains *aco1Δ*, *cyt2Δ*, and *sod1Δ* (B) were transformed with the reporter plasmid pCYC1-GFP. Strains were grown in minimal (SD) medium to repress *ATM1*, *YAH1*, *SSQ1*, and *HEM15* in the corresponding Gal strains. *CYC1* promoter activities were determined by measuring the GFP-specific fluorescence emission of logarithmically grown cells. C, wild type cells and cells producing Aft1p from the inducible vector p414-MET3 (*AFT1*↑) harboring pCYC1-GFP were cultivated in SD medium in the absence (+Fe) or presence of 50  $\mu$ M bathophenanthroline (-Fe). Promoter activities were measured as in A. D, mitochondria were isolated from wild type cells grown in YPD medium with and without 80  $\mu$ M bathophenanthroline. The enzymatic activities of malate dehydrogenase (MDH), activities of aconitase (ACO), succinate dehydrogenase (SDH), cytochrome oxidase (COX), and ferrochelatase (FeCH) were determined. The activities of iron-deplete cells relative to iron-replete cells are depicted. E, wild type, depleted Gal-HEM15, *aco1Δ*, and cells overproducing Aft1p (*AFT1*↑) harboring the reporter plasmid pFET3-GFP were grown as in C, and the *FET3* promoter strength was determined as in A. F, promoter strength of *CYC1* in wild type strain BY4741 and *cth2Δ* cells (growth as in C) was determined as described in A. Error bars indicate the standard deviation ( $n \geq 8$ ).

of the *FET3* gene, a representative member of the iron regulon, in the respiration-deficient *aco1Δ* and Hem15p-depleted Gal-HEM15 cells. Although *FET3* was strongly induced by iron depletion or upon overproduction of Aft1p (Fig. 4E, 2nd, 4th, and 6th bars), neither deletion of *ACO1* nor depletion of Hem15p had any significant effect on *FET3* transcription levels under iron-replete conditions (3rd and 5th bars). Importantly, *FET3* remained inducible under iron limitation in depleted Gal-HEM15 cells. Apparently, the failure to induce *FET3* in the absence of heme is limited to very low cellular heme levels (54). These data show that respiratory defects in general do not significantly alter gene expression of the iron regulon.

In turn, the induction of the iron regulon did not significantly affect the transcriptional activity of respiratory genes, as the *CYC1* promoter remained repressible by iron deprivation upon overproduction of Aft1p (Fig. 4C). Aft1p is indirectly involved in the repression of iron-responsive genes under iron-limiting conditions through the induction of Cth2p that binds to iron-

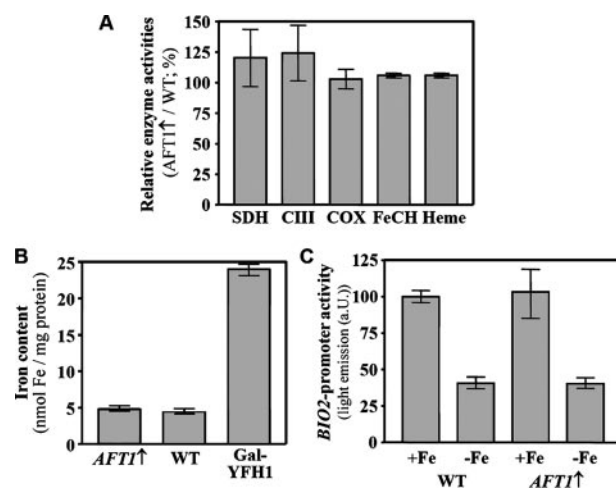


**FIGURE 5. The induction of *AFT1* does not affect mitochondrial iron metabolism.** Mitochondria were isolated from WT cells and cells overproducing Aft1p from vector p414-MET3 (*AFT1*↑) cultivated in SD medium. A, activities of succinate dehydrogenase (SDH), cytochrome *c* reductase (CIII), cytochrome oxidase (COX), and ferrochelatase (FeCH), and the cellular heme levels (see Fig. 6A) were determined. B, mitochondrial iron content was measured for wild type, *AFT1*↑, and Gal-YFH1 cells. C, promoter strength of *BIO2* in wild type and *AFT1*↑ cells grown under iron-replete (+Fe) and iron-deplete (-Fe) conditions was determined as described in Fig. 3E. Error bars indicate the standard deviation ( $n = 8$ ).

responsive mRNAs and facilitates their degradation (49). Indeed, under iron-limiting conditions, the GFP fluorescence generated from the pCYC1-GFP construct was slightly higher in *cth2Δ* and Aft1p-overproducing cells than in wild type (Fig. 4, C and F). However, the major part of the iron-responsive expression pattern of *CYC1* remained unchanged in *cth2Δ* cells demonstrating that the regulation of *CYC1* is largely independent of Cth2p alone (Fig. 4F). These results suggest that Aft1p or Aft1p-dependent genes are not the major factors governing the strong repression of *CYC1* (Fig. 2). This finding is in accordance with microarray data that show that genes involved in respiration are not affected upon overexpression of *AFT1* or *AFT2* (Fig. 1) (21). This lack of involvement of Aft1p in regulation of mitochondrial respiration was further supported by the observation that mitochondria isolated from Aft1p-overproducing cells showed wild type activities of the respiratory complexes II–IV (Fig. 5A). In addition, ferrochelatase activities and cellular heme levels were unchanged. Strikingly, mitochondria from Aft1p-overproducing cells showed no signs of iron accumulation, a general characteristic of ISC mutants (Fig. 5B). To investigate whether Aft1p is involved in the regulation of other iron-dependent mitochondrial processes, we analyzed the expression of *BIO2* in Aft1p-overproducing cells. Similar to *CYC1*, there was virtually no Aft1p-dependent change in the expression pattern of *BIO2* (Fig. 5C). This observation is in accordance with the microarray analyses of these cells (Fig. 1). Taken together, these data demonstrate that the activation of Aft1p plays no major role in the regulation of cellular respiration and other iron-related mitochondrial biosynthetic processes (Fig. 2). Aft1p/Aft2p induce the RNA-binding protein Cth2p, which has been shown to destabilize mRNAs encoding proteins involved in iron-dependent processes (49). Our data suggest that Aft1p activation alone does not suffice to fully



## Response to Fe/S Protein Maturation Defects in Yeast

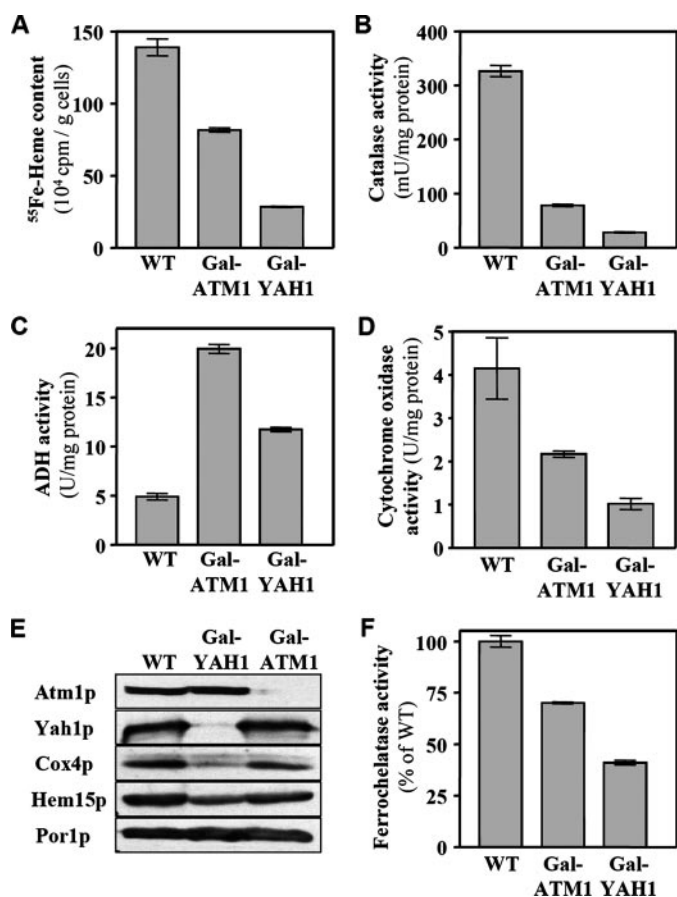


**FIGURE 6. Depletion of Yah1p and Atm1p impairs activities of heme-containing proteins and results in diminished heme pools.** A, WT and depleted Gal-ATM1 or Gal-YAH1 cells were cultivated for 16 h in SD medium supplemented with 10  $\mu$ Ci of  $^{55}\text{FeCl}_3$  and 1 mM ascorbate. Cells were harvested and  $^{55}\text{Fe}$ -heme was quantified as described in Ref. 34. Enzyme activities of catalase (B) or alcohol dehydrogenase (C) were measured in post-mitochondrial supernatants from WT and Gal-ATM1 or Gal-YAH1 cells grown in SD medium for 40 h (Gal-ATM1) and 48 h (Gal-YAH1). Enzyme activities of cytochrome c oxidase (D) were determined from isolated mitochondria. E, mitochondria from WT, depleted Gal-YAH1, and Gal-ATM1 cells were analyzed by immunoblotting using polyclonal sera directed against the indicated proteins. F, ferrochelatase activities of isolated mitochondria were determined from the insertion of endogenous  $\text{Zn}^{2+}$  into protoporphyrin IX (38). Error bars represent the standard deviation ( $n = 8$ ).

induce the functional activity of Cth2p thus requiring further studies to resolve this issue.

**Heme Deficiency Contributes to the Regulation of Genes for Heme-containing Proteins in Yah1p-depleted, but Not in Atm1p-depleted, Cells**—Cells depleted of Yah1p or Atm1p show a transcriptional deregulation of several heme-containing proteins and components involved in heme metabolism (Fig. 1 and Table 1). This effect may in part be caused by heme deficiency that is likely caused by the transcriptional repression of *HEM15* encoding ferrochelatase (Fig. 3A). To explore this possibility, we determined the steady state levels of cellular heme. Cells were cultivated for 16 h in minimal medium supplemented with  $^{55}\text{Fe}$ , and radioactive heme was extracted into an organic solvent to allow its quantification (29, 55). Under the conditions of the microarray experiments, the amount of radioactive heme was lower in cells depleted of Yah1p and Atm1p than in the wild type (Fig. 6A). The activity of catalase, a heme-dependent protein localized to the cytosol and peroxisomes,

was 3.5-fold lower in Atm1p-depleted cells than in wild type cells and almost undetectable in cells depleted of Yah1p (Fig. 6B). In addition, the activity of respiratory complex IV was 4- and 2-fold lower in cells depleted of Yah1p and Atm1p, respectively, whereas that of alcohol dehydrogenase increased (Fig. 6, C and D). Decreased complex IV activities correlated with diminished protein levels of Cox4p in both mutants (Fig. 6E). The reduced activities of these heme-containing enzymes correlated with the reduction of cellular heme contents, indicating that a lack of heme is a likely cause for the reduced activities of heme-containing enzymes in cells depleted of Yah1p and Atm1p. Reduced heme levels likely contribute to the transcriptional repression of heme-containing proteins, especially those that are under the control of the heme-dependent transcriptional activator Hap1p (56, 57). In Gal-YAH1 cells, *HAP1* was induced 4.4-fold (Table 1). Despite this induction, several genes that are regulated by Hap1p, such as *CTT1* or *YHB1*, were repressed rather than induced (supplemental Table SII). Because Hap1p requires heme for activity, low levels of heme in the Gal-YAH1 mutant most likely prevent Hap1p from activating the transcription of its target genes.

Although the heme deficiency of Gal-YAH1 cells detected under the conditions of the microarray experiment was expected from previous results, the partial heme deficiency of the ISC export mutant Gal-ATM1 came as a surprise, as it contradicted our own previous observations that indicated that the depletion of Atm1p in Gal-ATM1 cells is not associated with any significant loss of ferrochelatase function nor heme deficiency (8, 29). These earlier observations were made with cells cultivated in rich rather than minimal medium. Indeed, upon cultivation in rich medium, the low complex IV activities of Gal-ATM1 cells and other heme defects were not detectable (supplemental Fig. S1) (29). This observation suggests that the heme-deficient phenotype of Gal-ATM1 cells is a secondary consequence of Atm1p depletion that is observed only upon growth in minimal medium, which results in a stronger depletion of Atm1p compared with growth in rich medium. *atm1* $\Delta$  cells were originally identified in a genetic screen for mutants with defects in *c*-type cytochrome formation (39), indicating that cells deficient in Atm1p eventually develop a heme defect. This defect was found to be a secondary consequence caused by the oxidative damage of heme (39).

The change of the heme levels in the Gal-ATM1 mutant cultivated in different growth media (supplemental Fig. S1) opened the possibility to define which of the transcriptional responses were heme-dependent in this mutant. We carried out microarray analyses of Gal-ATM1 and wild type cells cultivated in rich medium (YPD). The transcriptomes of Atm1p-depleted Gal-ATM1 cells cultivated in rich or minimal medium were qualitatively rather similar (supplemental Table SIII). The response in rich medium was generally weaker, and many genes dropped below the threshold of a 2-fold change. This was the case for genes involved in mating type response, glucose fermentation, and the tricarboxylic acid cycle and most genes of amino acid metabolism. In accordance with the maintenance of heme-containing enzymes in rich medium (see above), *HEM15* encoding ferrochelatase was less depleted (fold change  $-1.76$ ) in rich than in minimal medium (fold change  $-2.87$ ). Remark-

ably, the transcriptional response of genes involved in respiration and heme metabolism showed no clear trend, as about half of the genes was increased whereas the other half was decreased in rich medium. This indicates that cellular heme levels in Gal-ATM1 cells play only a minor role in the transcriptional regulation of genes encoding heme-containing proteins or proteins involved in respiration. This strongly suggests that the transcriptional response to defects in the mitochondrial ISC export system results from the loss of a regulatory signal, and it is not a direct response to a respiratory- or heme-deficient phenotype. In cells with a compromised mitochondrial ISC assembly system, however, both heme deficiency and the loss of this regulatory signal contribute to the transcriptional response.

**No Detectable Heme Degradation by *Hmx1p* in *Atm1p*- and *Yah1p*-depleted Cells**—The decrease in cellular heme content upon depletion of *Atm1p* or *Yah1p* may be the result of a reduced heme synthesis or an increased degradation. A reduced synthesis was indicated by the transcriptional repression of *HEM15* encoding the ferrochelatase (Fig. 3A). Accordingly, protein levels of ferrochelatase were slightly reduced in the *ATM1* mutant, and a more pronounced decrease was found in the *YAH1* mutant (Fig. 6, E and F). These data suggest that the diminished heme content in Fe/S protein biogenesis mutants is likely caused by a decreased heme synthesis. On the other hand, an increased degradation of heme was also indicated by the fact that our microarray analysis indicated an induction of *HMX1* in ISC mutants (Table 1). *Hmx1p*, a heme-binding peroxidase involved in the degradation of heme, is an Aft1p target that is induced upon iron starvation, presumably to liberate iron from intracellular heme pools (55, 58, 59). Northern blot analysis confirmed the strong induction of *HMX1* mRNA levels in cells depleted of *Atm1p* or *Yah1p* and in iron-depleted wild type cells (Fig. 7A). To directly analyze the effect of heme degradation by *Hmx1p* on the cellular heme content, we determined the steady state levels of heme in the presence of different amounts of *Hmx1p* by radiolabeling of yeast cells with  $^{55}\text{FeCl}_3$ . In wild type cells, heme levels were altered only marginally (~1.5-fold) upon deletion or overexpression of *HMX1* (Fig. 7B) (55). In addition, the deletion of *hmx1* in Gal-*ATM1* and Gal-*YAH1* backgrounds had no significant effects on the heme content of these cells under depleting conditions (Fig. 7C). These findings rule out a major role of *Hmx1p* in heme degradation as an explanation for the low cellular heme contents. We therefore conclude that the heme deficiency observed in mutants with defects in the mitochondrial ISC assembly and export apparatus are explained by a decreased heme synthesis caused by low levels of active ferrochelatase. This low activity is caused in part by a transcriptional repression of *HEM15*, an iron-responsive gene in *S. cerevisiae* (48). Thus, the artificial iron-deprivation status prevailing in cells with defects in the mitochondrial ISC assembly and export systems also contributes to heme deficiency, which is generally found in these cells. In addition, ferrochelatase is inhibited biochemically in response to a defective Fe/S protein biogenesis (29). Thus, transcriptional and post-transcriptional mechanisms contribute to the heme deficiency in cells with defects in the mitochondrial ISC assembly and export systems.

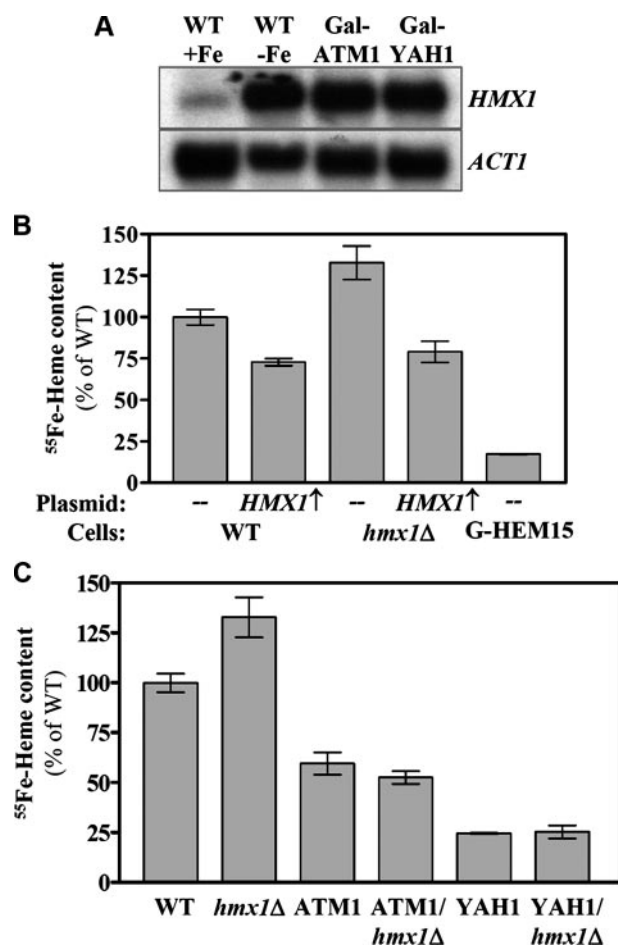


**FIGURE 7. Impaired heme levels in cells with defective ISC machineries are not because of heme degradation.** A, Northern blot analysis of *HMX1*. Total RNA of WT cells cultivated overnight without (+Fe) or with 50  $\mu\text{M}$  bathophenanthroline (-Fe) and of depleted Gal-*ATM1* or Gal-*YAH1* cells was separated on agarose gels, blotted onto nylon membrane, and hybridized to a  $^{32}\text{P}$ -labeled probe for *HMX1* and *ACT1*. B, WT or *hmx1*Δ cells harboring either plasmid p426-*HMX1* (*HMX1*↑) or the empty vector and Gal-*HEM15* cells (G-*HEM15*) were grown in SD medium supplemented with  $^{55}\text{FeCl}_3$  for 16 h, and the cellular  $^{55}\text{Fe}$ -heme content was determined as described in Fig. 6A. C, cellular heme content of WT or *hmx1*Δ cells and the mutants Gal-*ATM1* (*ATM1*), Gal-*YAH1* (*YAH1*), Gal-*ATM1/hmx1*Δ (*ATM1/hmx1*Δ), and Gal-*YAH1/hmx1*Δ (*YAH1/hmx1*Δ) was determined as described above ( $n \geq 8$ ).

## DISCUSSION

In this study, we have performed a comparative analysis of the global transcriptional consequences of functional defects in the three cellular Fe/S protein biogenesis systems in *S. cerevisiae*. Defects in mitochondrial Fe/S protein maturation are associated with a substantial accumulation of iron within the mitochondria and the constitutive expression of the yeast iron regulon, observations that indicated a de-regulation of cellular iron homeostasis (18, 19, 29, 60). Our systematic analyses considerably extend this conclusion in that they revealed that yeast cells depleted of members of the mitochondrial ISC assembly and export apparatus show strong and largely similar transcriptional responses, which substantially overlap with the transcriptional response of yeast to iron deprivation (48, 49, 61). Thus, yeast cells with defects in the mitochondrial ISC assembly and export systems resemble, on the transcriptional level, iron-starved cells suggesting that the mitochondrial ISC systems are major sensors and regulators for cellular iron homeo-

## Response to Fe/S Protein Maturation Defects in Yeast

stasis (Fig. 2). Virtually all iron-dependent cellular pathways are transcriptionally remodeled upon defects in the ISC systems. Importantly, the constitutive activation of the Aft1/2p transcription factors does not suffice to elicit the full response seen upon iron starvation or after ISC assembly and export defects (Fig. 1). For instance, the repression of respiration and heme biosynthesis and the induction of the sterol pathway is not part of the Aft regulon. Because iron starvation of cells decreases the activity of the mitochondrial ISC pathways, the iron-deplete condition is likely sensed by the ISC systems that in turn activate appropriate adaptive responses for improved iron acquisition, properly balanced use of iron between heme, Fe/S cluster synthesis, and other iron-connected processes (Fig. 2).

Even though iron regulation in higher eukaryotes differs substantially from that in yeast (4–7), the regulatory role of the ISC systems is most likely conserved in vertebrates, as mice or humans depleted of Abcb7 and patients suffering from low levels of frataxin display an iron accumulation in affected tissues (62, 63). In addition, defects in the mitochondrial ISC member Grx5p induce an altered iron homeostasis in zebrafish (64).

The transcriptional profile of cells depleted of the CIA member Nbp35p did not show any response that would link cytosolic Fe/S protein biogenesis to cellular iron homeostasis. Preliminary microarray analyses of cells depleted of the CIA members Nar1p and Cia1p support this conclusion and confirm the previous observation in that the disruption of the cytosolic Fe/S protein biogenesis system is not associated with a constitutive induction of the iron regulon despite the strong inhibition of cytosolic or nuclear Fe/S protein assembly (16, 26). These findings indicate that iron sensing in the cytosol by iron-responsive proteins such as Aft1/2p is not regulated by binding of an Fe/S cluster or by interaction with a canonical Fe/S protein. Because the constitutive transcriptional activation of the iron regulon in mutants with defects in mitochondrial Fe/S protein maturation is largely independent of the status of cytosolic iron (25, 26), it is clear that the regulatory function is executed by the mitochondrial ISC assembly and export machineries (Fig. 2). The transcriptional profiles reported for cells depleted of other ISC members, Grx5p and Nfs1p, were rather similar to those of our Yah1p-depleted cells; however, those array data were not analyzed in depth (18, 19, 65). Collectively, these results strongly suggest that the induction of the iron-deprivation response seen in Yah1p-depleted cells is most likely typical for all cells with defects in the mitochondrial ISC assembly system. Our promoter studies with cells depleted of the specialized mitochondrial Hsp70 chaperone Ssq1p further substantiate this conclusion.

Besides the induction of cellular iron uptake systems, the transcriptional response of yeast to iron deprivation encompasses the transcriptional remodeling of central mitochondrial functions, including respiration and the citric acid cycle, and the remodeling of several key biosynthetic pathways, including those for ergosterol, biotin, and several amino acids (48, 49, 53, 66). The iron-responsive transcription factors Aft1p and Aft2p are responsible only for the induction of the iron regulon in response to iron deficiency. There is no evidence that these transcription factors are also directly involved in the regulation of other iron-responsive genes (Fig. 1) (21, 22, 53, 66, 67). The

iron regulon includes the RNA-binding protein Cth2p that modulates the mRNA stability of several iron-dependent genes. However, the transcriptional profile reported for a *cth2Δ* strain displayed only moderate changes in the expression of iron-responsive genes, indicating that in most cases the contribution of Cth2p may be a fine-tuning of the massive transcriptional repression of respiratory genes under iron-limiting conditions (49). Our analysis is consistent with this conclusion as it shows that neither the constitutive overproduction of Aft1p nor *cth2* deletion has a significant effect on the iron-dependent transcription of *CYC1*, the respiratory gene which shows the strongest iron response in *S. cerevisiae*. In addition, cells overproducing Aft1p show no signs of mitochondrial dysfunction, despite the fact that these cells strongly induce Cth2p. However, several of the respiratory genes repressed in cells depleted of Atm1p or Yah1p contain Cth2p-binding sites (49). Thus, the regulatory effects of Cth2p may vary for individual genes thus requiring a more comprehensive analysis. Taken together, although Aft1p indirectly contributes to the transcriptional repression of iron-responsive genes under iron-limiting conditions, Aft1p does not play a decisive role in the regulation of a large number of iron-responsive pathways.

The expression of respiratory genes is modulated by several key processes, including a shift in carbon source, cellular oxygen levels, oxidative stress, and mitochondrial dysfunctions that result in respiratory deficiency (45, 53, 66, 68). Defects in mitochondrial ISC assembly result in glutamate deficiency that triggers the retrograde response, the physiological response of yeast to mitochondrial dysfunctions (44, 45, 47). The retrograde response is activated in the ISC assembly mutant Gal-YAH1 most likely because of low levels of functional aconitase. In the ISC export mutant Gal-ATM1 normal aconitase activities are found, and consequently the corresponding response is absent (Table 1). A switch to fermentation is associated with the transcriptional repression of respiratory genes, a process in which the transcriptional activator complex Hap2–5p plays a major role (69, 70). In Atm1p- and Yah1p-depleted cells, this switch to fermentation is indicated by the induction of genes involved in glucose utilization and uptake. Low levels of heme result in transcriptional repression of respiratory genes. In *S. cerevisiae*, heme functions as an indirect indicator for ambient oxygen levels and is sensed by the heme-activated transcription factor Hap1p that regulates the transcriptional adaptation to anoxic conditions (56, 57). Typical Hap1p-regulated genes are repressed in depleted Gal-ATM1 and Gal-YAH1 cells, although Hap1p is induced. A similar repression of Hap1p-regulated genes is seen upon iron deprivation (49). How Hap1p, the Hap2–5p complex, and other transcription factors integrate the iron-responsive expression of respiratory genes in wild type and ISC-compromised cells remains to be determined.

In *S. cerevisiae*, disruption of the mitochondrial ISC assembly system is generally associated with decreased heme levels and a severe cytochrome deficiency (27–29, 71). Functional impairment of the mitochondrial ISC assembly system induces the accumulation of a regulatory substance within mitochondria that causes a reversible inhibition of ferrochelatase (29). Our transcriptional studies now add a further regulatory connection between heme synthesis and Fe/S cluster biogenesis. *HEM15*,



the gene encoding the enzyme ferrochelatase that catalyzes the insertion of iron into protoporphyrin IX, is repressed in cells with defects in the mitochondrial ISC assembly and export apparatus by a similar margin as under low iron conditions. A reduced synthesis of heme fully explains the heme deficiency of ISC mutants. Our results show that degradation of heme may only marginally contribute to the observed low cellular heme levels, even though *HMX1*, an iron-responsive gene encoding a heme-binding peroxidase, was induced (55). Thus, the deregulated cellular iron homeostasis prevailing in cells with defects in the mitochondrial ISC assembly and export systems also impacts on cellular heme levels (Fig. 2). As a consequence, low cellular heme levels may contribute significantly to the transcriptional changes observed in iron-starved cells or in cells with defects in mitochondrial Fe/S protein maturation. The resulting transcriptional repression of heme-dependent genes and genes involved in respiration, in turn, may aggravate the heme and respiratory deficiency in a vicious cycle. The coordinated regulation of the ISC and heme biosynthesis pathways ensures balanced use of iron in these processes and thus is of central physiological relevance. Taken together, the status of the mitochondrial ISC assembly machinery regulates the cellular levels of heme by two independent mechanisms, the transcriptional regulation of cellular ferrochelatase levels and the biochemical regulation of the enzymatic activities of ferrochelatase via a mitochondrial soluble inhibitor (Fig. 2).

Remarkably, only the last step of the biosynthesis of heme is regulated by iron in yeast. *HEM15* is the only gene involved in the biosynthesis of heme that is repressed upon iron limitation (48, 49). Genes involved in the biosynthesis of the porphyrin ring are regulated neither by iron deficiency nor by defects in cellular Fe/S maturation. In addition, cellular heme levels do not affect the uptake of iron at the plasma membrane as heme deficiency is not associated with an induction of the iron regulon (Fig. 2). In fact, heme-deficient cells altogether fail to induce several genes of the iron regulon under iron-deficient conditions (54). Thus, although cellular heme levels may influence the expression of genes involved in respiration and ergosterol biosynthesis, heme does not regulate the expression of iron-responsive genes in yeast, in contrast to what is found for the mitochondrial ISC assembly and export systems.

In summary, our study provides the first comprehensive analysis of the global consequences of defects in all three Fe/S cluster biogenesis systems in a comparative fashion. Our analysis demonstrates that mitochondria, the major consumers of iron in the cell, play a central role in the regulation of numerous processes connected to cellular iron metabolism and other iron-linked pathways. The mitochondrial ISC assembly and export systems function as major cellular devices for the sensing of iron by regulating iron-responsive gene expression and the control of cellular heme levels in *S. cerevisiae*. Our data support the conclusion that the mitochondrial ISC assembly and export systems produce and sequester a key molecule that functions as a regulatory signal for gene expression of a complex network of numerous iron and heme-linked biochemical pathways (Fig. 2). The identification of this regulatory signal is central for understanding the mechanism underlying the regu-

latory cross-talks between mitochondrial Fe/S protein biogenesis, heme synthesis, and iron-responsive gene expression.

*Acknowledgments*—We thank Dr. Martin Eilers for access to the microarray equipment, Dr. Dennis Winge for access to original microarray data, and Dr. Heike Krebber for the kind gift of plasmid *pPS1372*.

## REFERENCES

1. Beinert, H., Holm, R. H., and Munck, E. (1997) *Science* **277**, 653–659
2. Beinert, H. (2000) *J. Biol. Inorg. Chem.* **5**, 2–15
3. Johnson, D. C., Dean, D. R., Smith, A. D., and Johnson, M. K. (2005) *Annu. Rev. Biochem.* **74**, 247–281
4. Craig, E. A., and Marszalek, J. (2002) *Cell. Mol. Life Sci.* **59**, 1658–1665
5. Lill, R., and Muhlenhoff, U. (2005) *Trends Biochem. Sci.* **30**, 133–141
6. Rouault, T. A., and Tong, W. H. (2005) *Nat. Rev. Mol. Cell Biol.* **6**, 345–351
7. Lill, R., and Muhlenhoff, U. (2006) *Annu. Rev. Cell Dev. Biol.* **22**, 457–486
8. Kispal, G., Csere, P., Prohl, C., and Lill, R. (1999) *EMBO J.* **18**, 3981–3989
9. Muhlenhoff, U., Balk, J., Richhardt, N., Kaiser, J. T., Sipos, K., Kispal, G., and Lill, R. (2004) *J. Biol. Chem.* **279**, 36906–36915
10. Biederbick, A., Stehling, O., Rosser, R., Niggemeyer, B., Nakai, Y., Elsasser, H. P., and Lill, R. (2006) *Mol. Cell. Biol.* **26**, 5675–5687
11. Lange, H., Lisowsky, T., Gerber, J., Muhlenhoff, U., Kispal, G., and Lill, R. (2001) *EMBO Rep.* **2**, 715–720
12. Sipos, K., Lange, H., Fekete, Z., Ullmann, P., Lill, R., and Kispal, G. (2002) *J. Biol. Chem.* **277**, 26944–26949
13. Roy, A., Solodovnikova, N., Nicholson, T., Antholine, W., and Walden, W. E. (2003) *EMBO J.* **22**, 4826–4835
14. Balk, J., Pierik, A. J., Netz, D. J., Muhlenhoff, U., and Lill, R. (2004) *EMBO J.* **23**, 2105–2115
15. Hausmann, A., Aguilar Netz, D. J., Balk, J., Pierik, A. J., Muhlenhoff, U., and Lill, R. (2005) *Proc. Natl. Acad. Sci. U. S. A.* **102**, 3266–3271
16. Balk, J., Aguilar Netz, D. J., Pepper, K., Pierik, A. J., and Lill, R. (2005) *Mol. Cell. Biol.* **25**, 10833–10841
17. Yamaguchi-Iwai, Y., Stearman, R., Dancis, A., and Klausner, R. D. (1996) *EMBO J.* **15**, 3377–3384
18. Foury, F., and Talibi, D. (2001) *J. Biol. Chem.* **276**, 7762–7768
19. Belli, G., Molina, M. M., Garcia-Martinez, J., Perez-Ortin, J. E., and Hertero, E. (2004) *J. Biol. Chem.* **279**, 12386–12395
20. Yamaguchi-Iwai, Y., Dancis, A., and Klausner, R. D. (1995) *EMBO J.* **14**, 1231–1239
21. Rutherford, J. C., Jaron, S., and Winge, D. R. (2003) *J. Biol. Chem.* **278**, 27636–27643
22. Rutherford, J. C., and Bird, A. J. (2004) *Eukaryot. Cell* **3**, 1–13
23. Dubacq, C., Chevalier, A., Courbeyrette, R., Petat, C., Gidrol, X., and Mann, C. (2006) *Mol. Genet. Genomics* **275**, 114–124
24. Yamaguchi-Iwai, Y., Ueta, R., Fukunaka, A., and Sasaki, R. (2002) *J. Biol. Chem.* **277**, 18914–18918
25. Chen, O. S., Crisp, R. J., Valachovic, M., Bard, M., Winge, D. R., and Kaplan, J. (2004) *J. Biol. Chem.* **279**, 29513–29518
26. Rutherford, J. C., Ojeda, L., Balk, J., Muhlenhoff, U., Lill, R., and Winge, D. R. (2005) *J. Biol. Chem.* **280**, 10135–10140
27. Lesuisse, E., Santos, R., Matzanke, B. F., Knight, S. A., Camadro, J. M., and Dancis, A. (2003) *Hum. Mol. Genet.* **12**, 879–889
28. Santos, R., Buisson, N., Knight, S. A., Dancis, A., Camadro, J. M., and Lesuisse, E. (2004) *Mol. Microbiol.* **54**, 507–519
29. Lange, H., Muhlenhoff, U., Denzel, M., Kispal, G., and Lill, R. (2004) *J. Biol. Chem.* **279**, 29101–29108
30. Sherman, F. (2002) *Methods Enzymol.* **350**, 3–41
31. Yang, Y. H., Dudoit, S., Luu, P., Lin, D. M., Peng, V., Ngai, J., and Speed, T. P. (2002) *Nucleic Acids Res.* **30**, e15
32. Sambrook, J., and Russel, D. W. (2001) *Molecular Cloning: A Laboratory Manual*, 3rd Ed., Cold Spring Harbor Laboratory Press, Cold Spring Harbor, NY
33. Taura, T., Krebber, H., and Silver, P. A. (1998) *Proc. Natl. Acad. Sci. U. S. A.* **95**, 7427–7432

## Response to Fe/S Protein Maturation Defects in Yeast

34. Lange, H., Kispal, G., and Lill, R. (1999) *J. Biol. Chem.* **274**, 18989–18996
35. Gietz, R. D., and Woods, R. A. (2002) *Methods Enzymol.* **350**, 87–96
36. Diekert, K., de Kroon, A. I., Kispal, G., and Lill, R. (2001) *Methods Cell Biol.* **65**, 37–51
37. Harlow, E., and Lane, D. (1988) *Antibodies: A Laboratory Manual*, Cold Spring Harbor Laboratory Press, Cold Spring Harbor, NY
38. Camadro, J. M., and Labbe, P. (1988) *J. Biol. Chem.* **263**, 11675–11682
39. Kispal, G., Csere, P., Guiard, B., and Lill, R. (1997) *FEBS Lett.* **418**, 346–350
40. Lange, H., Kaut, A., Kispal, G., and Lill, R. (2000) *Proc. Natl. Acad. Sci. U. S. A.* **97**, 1050–1055
41. Pennaneach, V., Putnam, C. D., and Kolodner, R. D. (2006) *Mol. Microbiol.* **59**, 1357–1368
42. Lesur, I., and Campbell, J. L. (2004) *Mol. Biol. Cell* **15**, 1297–1312
43. DeRisi, J. L., Iyer, V. R., and Brown, P. O. (1997) *Science* **278**, 680–686
44. Butow, R. A., and Avadhani, N. G. (2004) *Mol. Cell* **14**, 1–15
45. Liu, Z., and Butow, R. A. (2006) *Annu. Rev. Genet.* **40**, 159–185
46. Knight, S. A., Sepuri, N. B., Pain, D., and Dancis, A. (1998) *J. Biol. Chem.* **273**, 18389–18393
47. Epstein, C. B., Waddle, J. A., Hale, W. T., Dave, V., Thornton, J., Macatee, T. L., Garner, H. R., and Butow, R. A. (2001) *Mol. Biol. Cell* **12**, 297–308
48. Shakoury-Elizeh, M., Tiedeman, J., Rashford, J., Ferea, T., Demeter, J., Garcia, E., Rolfes, R., Brown, P. O., Botstein, D., and Philpott, C. C. (2004) *Mol. Biol. Cell* **15**, 1233–1243
49. Puig, S., Askeland, E., and Thiele, D. J. (2005) *Cell* **120**, 99–110
50. Rosenfeld, E., and Beauvoit, B. (2003) *Yeast* **20**, 1115–1144
51. Barros, M. H., Nobrega, F. G., and Tzagoloff, A. (2002) *J. Biol. Chem.* **277**, 9997–10002
52. Hinnebusch, A. G. (2005) *Annu. Rev. Microbiol.* **59**, 407–450
53. Kaplan, J., McVey Ward, D., Crisp, R. J., and Philpott, C. C. (2006) *Biochim. Biophys. Acta* **1763**, 646–651
54. Crisp, R. J., Adkins, E. M., Kimmel, E., and Kaplan, J. (2006) *EMBO J.* **25**, 512–521
55. Protchenko, O., and Philpott, C. C. (2003) *J. Biol. Chem.* **278**, 36582–36587
56. Kwast, K. E., Burke, P. V., Staahl, B. T., and Poyton, R. O. (1999) *Proc. Natl. Acad. Sci. U. S. A.* **96**, 5446–5451
57. Zhang, L., and Hach, A. (1999) *Cell. Mol. Life Sci.* **56**, 415–426
58. Santos, R., Buisson, N., Knight, S., Dancis, A., Camadro, J. M., and Lesuisse, E. (2003) *Microbiology* **149**, 579–588
59. Kim, D., Yukl, E. T., Moenne-Loccoz, P., and Montellano, P. R. (2006) *Biochemistry* **45**, 14772–14780
60. Chen, O. S., Hemenway, S., and Kaplan, J. (2002) *Proc. Natl. Acad. Sci. U. S. A.* **99**, 12321–12326
61. Lan, C. Y., Rodarte, G., Murillo, L. A., Jones, T., Davis, R. W., Dungan, J., Newport, G., and Agabian, N. (2004) *Mol. Microbiol.* **53**, 1451–1469
62. Pondarre, C., Antiochos, B. B., Campagna, D. R., Clarke, S. L., Greer, E. L., Deck, K. M., McDonald, A., Han, A. P., Medlock, A., Kutok, J. L., Anderson, S. A., Eisenstein, R. S., and Fleming, M. D. (2006) *Hum. Mol. Genet.* **15**, 953–964
63. Popescu, B. F., Pickering, I. J., George, G. N., and Nichol, H. (2007) *J. Inorg. Biochem.* **101**, 957–966
64. Wingert, R. A., Galloway, J. L., Barut, B., Foott, H., Fraenkel, P., Axe, J. L., Weber, G. J., Dooley, K., Davidson, A. J., Schmid, B., Paw, B. H., Shaw, G. C., Kingsley, P., Palis, J., Schubert, H., Chen, O., Kaplan, J., and Zon, L. I. (2005) *Nature* **436**, 1035–1039
65. Mnaimneh, S., Davierwala, A. P., Haynes, J., Moffat, J., Peng, W. T., Zhang, W., Yang, X., Pootoolal, J., Chua, G., Lopez, A., Trochesset, M., Morse, D., Krogan, N. J., Hiley, S. L., Li, Z., Morris, Q., Grigull, J., Mitsakakis, N., Roberts, C. J., Greenblatt, J. F., Boone, C., Kaiser, C. A., Andrews, B. J., and Hughes, T. R. (2004) *Cell* **118**, 31–44
66. Kwok, E., and Kosman, D. J. (2005) in *Topics in Current Genetics* (Tamás, M. J., and Martinoia, E., eds) pp. 59–100, Springer-Verlag, Berlin
67. Masse, E., and Arguin, M. (2005) *Trends Biochem. Sci.* **30**, 462–468
68. McCammon, M. T., Epstein, C. B., Przybyla-Zawislak, B., McAlister-Henn, L., and Butow, R. A. (2003) *Mol. Biol. Cell* **14**, 958–972
69. Schuller, H. J. (2003) *Curr. Genet.* **43**, 139–160
70. Gancedo, J. M. (1998) *Microbiol. Mol. Biol. Rev.* **62**, 334–361
71. Zhang, Y., Lyver, E. R., Knight, S. A., Lesuisse, E., and Dancis, A. (2005) *J. Biol. Chem.* **280**, 19794–19807

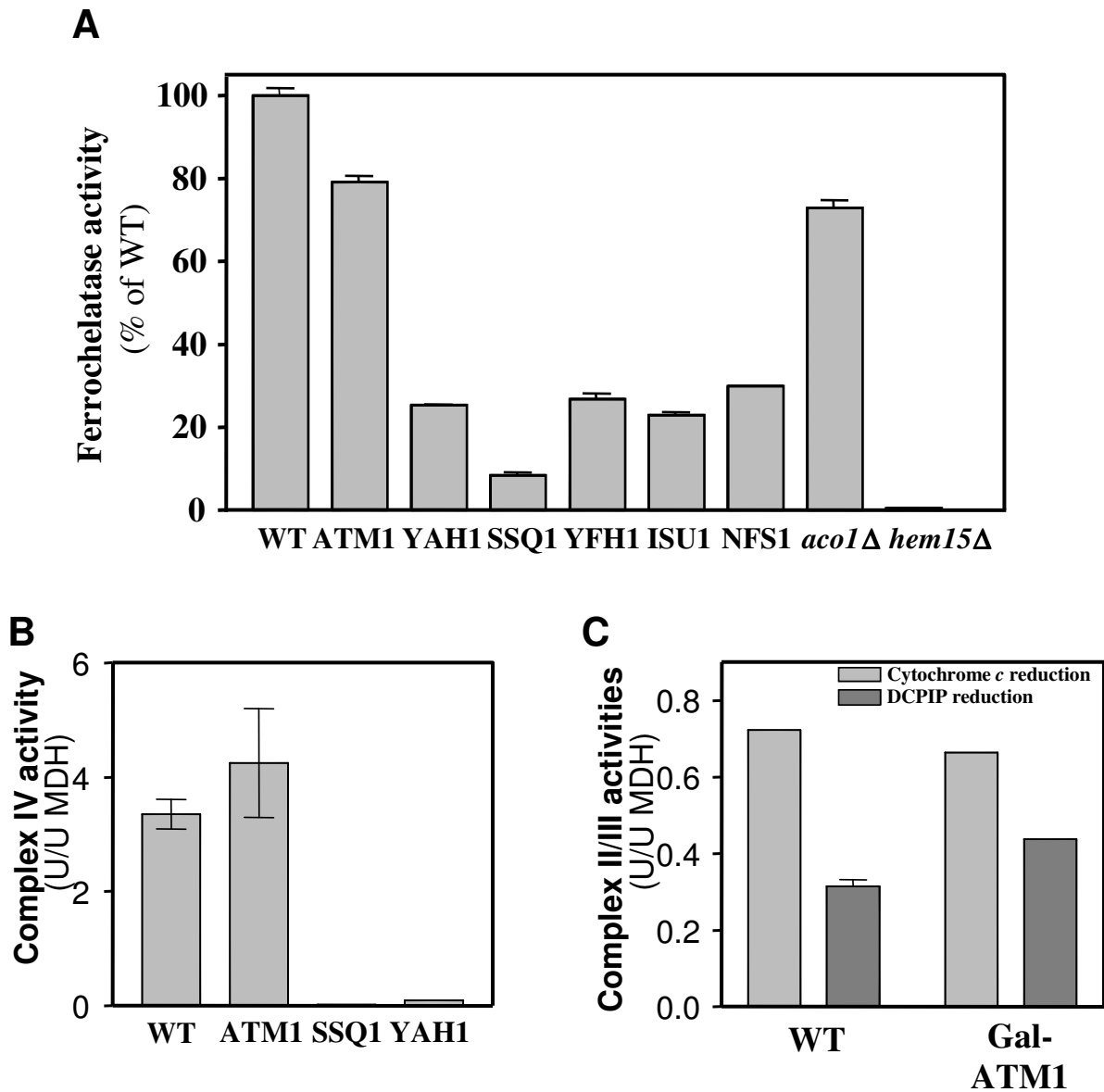


**Fig. S1: Depletion of Atm1p in rich medium does not affect activities of heme-dependent proteins.** Mitochondria were isolated from wild type (WT), the indicated conditional Gal-ISC strains, *aco1*Δ and *hem15*Δ cells cultivated in rich (YP) medium supplemented with glucose. (A) Ferrochelatase activities of isolated mitochondria were determined from the insertion of endogenous Zn<sup>2+</sup> into protoporphyrin IX. Enzyme activities of complexes IV (B), complex II or complexes II plus III (C) were determined from the rates of cytochrome *c* oxidation (B), DCPIP-reduction and cytochrome *c* reduction (C), respectively. Enzyme activities were normalized to the activity of malate dehydrogenase (MDH).



**CELLULAR AND MITOCHONDRIAL REMODELLING UPON DEFECTS IN IRON-SULFUR  
PROTEIN BIOGENESIS**

Anja Hausmann, Birgit Samans, Roland Lill and Ulrich Mühlenhoff

**SUPPLEMENT**

**Note:** For the complete set of microarray data see:

<http://www.uni-marburg.de/fb20/cyto/Muehlenhoff/research>.

Raw microarray data are available from ArrayExpress at EBI, accession number E-MEXP-1215.

**Supplementary Table SI**  
Selected genes induced or repressed upon depletion of the CIA-factor Nbp35p.

<b>ORF</b>	<b>Gene</b>	<b>Description</b>	<b>Average fold change</b>
<b>Y-elements</b>			
YEL075C		Similar to other subtelomerically-encoded proteins	1,72
YGR296W		Similar to other subtelomerically-encoded proteins	1,67
YHL050C		Similar to other subtelomerically-encoded proteins	2,00
YIL177C		Similar to other subtelomerically-encoded proteins	-1,56
YLR464W		Similar to other subtelomerically-encoded proteins	1,98
YLR466W	<i>YRF1</i>	Y' helicase (subtelomerically-encoded)	1,80
YML133C		Similar to other subtelomerically-encoded proteins	1,92
YNR075W	<i>COS10</i>	Similar to other subtelomerically-encoded proteins	1,63
YPR202W		Similar to other subtelomerically-encoded proteins	1,89
YPR203W		Similar to other subtelomerically-encoded proteins	1,78
YPR204W		Similar to other subtelomerically-encoded proteins	2,10
<b>Mitochondrial ribosomal subunits</b>			
YDR041W	<i>RSM10</i>	Ribosomal protein; mitochondrial	-1,73
YGL068W	<i>MNP1</i>	Similar to ribosomal proteins	-1,79
YBR282W	<i>MRPL27</i>	Ribosomal protein; mitochondrial L27	-1,74
YBR268W	<i>MRPL37</i>	Ribosomal protein; mitochondrial L37	-1,54
YKL170W	<i>MRPL38</i>	Ribosomal protein; mitochondrial L38	-1,61
YJL096W	<i>MRP149</i>	Ribosomal protein; mitochondrial large subunit	-1,62
<b>Glucose transport and fermentation</b>			
YHR096C	<i>HXT5</i>	Hexose permease	1,65
YNR072W	<i>HXT17</i>	Hexose permease	1,58
YPL061W	<i>ALD6</i>	Aldehyde dehydrogenase	1,93
<b>Respiration/TCA Cycle</b>			
YIL070C	<i>MAM33</i>	Mitochondrial acidic matrix protein (oxidative phosphorylation)	-1,71

YNL315C	<i>ATP11</i>	F1F0-ATPase complex assembly protein	-1,62
YJL180C	<i>ATP12</i>	F1F0-ATPase complex assembly (molecular chaperone)	-1,59
YKL141W	<i>SDH3</i>	Succinate dehydrogenase cytochrome b	-1,66
YCR005C	<i>CIT2</i>	Peroxisomal citrate synthase	1,88
<b>Iron responsive proteins</b>			
YMR319C	<i>FET4</i>	Iron transporter	-1,63
<b>Fe/S protein biogenesis</b>			
YOR226C	<i>ISU2</i>	Scaffold protein	1,52
<b>Sulfate assimilation / acquisition</b>			
YJR010W	<i>MET3</i>	ATP sulfurylase	1,57
YBR294W	<i>SUL1</i>	Sulfate permease	2,67
<b>Amino acid metabolism</b>			
YKL029C	<i>MAE1</i>	Precursor for synthesis of several amino acids	1,56
YDR368W	<i>YPR1</i>	2-methylbutyraldehyde reductase	-1,98
YBR068C	<i>BAP2</i>	Branched-chain amino acid permease	1,56
YDR046C	<i>BAP3</i>	Branched-chain amino acid permease	1,61
YDR508C	<i>GNP1</i>	Glutamine permease	1,66
YNL268W	<i>LYP1</i>	Lysine permease	1,61
YER081W	<i>SER3</i>	3-phosphoglycerate dehydrogenase	-1,72
<b>Mating</b>			
YDR461W	<i>MFA1</i>	A-factor precursor	-1,98
<b>Protein modification</b>			
YBR093C	<i>PHO5</i>	Repressible acid phosphatases	-2,10
YBR097W	<i>VPS15</i>	Serine/threonine protein kinase	-1,73
<b>Purine / pyrimidine biosynthesis</b>			
YAR015W	<i>ADE1</i>	N-succinyl-5-aminoimidazole-4-carboxamide ribotide synthetase	-1,77
YLR359W	<i>ADE13</i>	Adenylosuccinate lyase	-1,52
YMR120C	<i>ADE17</i>	5-aminoimidazole-4-carboxamide ribonucleotide transformylase	-1,94
YMR271C	<i>URA10</i>	Orotate phosphoribosyltransferase	-1,79
<b>Multidrug resistance transporter</b>			
YOR153W	<i>PDR5</i>	Multidrug resistance transporter	2,19

Fold changes are given in relation to those of the wild type cultivated under the same experimental conditions. Values are averages of two biological and technical experiments including dye swaps between experiment and reference sample. Repressed genes are indicated by a (-) sign. The cut-off level is 1.5.

**Supplementary Table SII**  
**Selected genes induced or repressed upon depletion of the mitochondrial ISC assembly component Yah1p or the ISC export component Atm1p.**

ORF	Gene	Description	Average fold change	
			Gal-YAH1	Gal-ATM1
<b>Iron regulon (Aft1p / Aft2p) / iron responsive proteins</b>				
<b>YHL040C</b>	<i>ARN1</i>	Siderophore transporter	33,7	16,5
YHL047C	<i>ARN2</i>	Siderophore transporter	52,52	30,11
<b>YEL065W</b>	<i>SIT1/ARN3</i>	Ferrioxamine B permease	5,97	4,06
<b>YOL158C</b>	<i>ENB1/ARN4</i>	Enterobactin transporter	14,61	14,52
<b>YNL259C</b>	<i>ATX1</i>	Copper metallochaperone		2,05
YDR270W*	<i>CCC2</i>	Cu(2+)-transporting ATPase	4,51	2,49
<b>YMR058W</b>	<i>FET3</i>	Cell surface ferroxidase	34,52	14,1
YMR319C	<i>FET4</i>	Iron transporter	3,49	
YFL041W	<i>FET5</i>	Multicopper oxidase	3,22	2,72
<b>YDR534C</b>	<i>FIT1</i>	Retention of siderophore iron	162	111
<b>YOR382W</b>	<i>FIT2</i>	Retention of siderophore iron	111,26	94,05
<b>YOR383C</b>	<i>FIT3</i>	Retention of siderophore iron	14,95	17,64
<b>YLR214W</b>	<i>FRE1</i>	Ferric (and cupric) reductase	5,10	5,84
<b>YKL220C</b>	<i>FRE2</i>	Ferric (and cupric) reductase	5,80	4,92
<b>YOR381W</b>	<i>FRE3</i>	Ferric reductase	6,30	4,73
<b>YOR384W</b>	<i>FRE5</i>	Putative ferric reductase	4,47	3,25
YBR207W	<i>FTH1</i>	Iron transporter		2,68
<b>YER145C</b>	<i>FTR1</i>	Iron permease	15,8	9,83
<b>YLR136C</b>	<i>CTH2</i>	mRNA degradation		2,93
<b>YDR264C</b>	<i>AKR1</i>	Palmitoyl transferase	2,86	3,12
<b>YDR271C</b>		Unknown		2,31
<b>YNR056C</b>	<i>BIO5</i>	Biotin synthesis	4,33	3,06
<b>YOR387C</b>		Unknown		-3,32
<b>YBR012C</b>		Unknown	7,07	
<b>YBR072W</b>	<i>HSP26</i>	Small heat shock protein	26,19	3,90
<b>YGR146C</b>		Unknown	4,76	
<b>YMR041C</b>		Unknown	2,95	
<b>YGR065C</b>	<i>VHT1</i>	Biotin transporter		4,79
<b>Fe/S protein biogenesis</b>				
YPL059W	<i>GRX5</i>	Glutathione-dependent oxidoreductase	-2,81	-2,21
<b>YPL135W</b>	<i>ISU1</i>	Scaffold protein	3,91	3,24
YOR226C	<i>ISU2</i>	Scaffold protein	4,01	2,15
<b>Respiration</b>				
YKL148C	<i>SDH1</i>	Succinate dehydrogenase flavoprotein subunit	-5,04	-3,29
YKL141W	<i>SDH3</i>	Succinate dehydrogenase cytochrome b	-3,43	-2,49
YDR178W	<i>SDH4</i>	Succinate dehydrogenase anchor subunit	-3,46	-2,50
YBL045C*	<i>COR1</i>	Ubiquinol cyt.-c reductase	-3,36	-2,35
YEL024W	<i>RIP1</i>	Ubiquinol cyt.-c reductase / Rieske Fe/S protein	-6,17	-4,83
YPR191W*	<i>QCR2</i>	Ubiquinol cyt.-c reductase core protein 2	-4,32	-2,83
YFR033C	<i>QCR6</i>	Ubiquinol cyt.-c reductase subunit		-2,12
YDR529C	<i>QCR7</i>	Ubiquinol cyt.-c reductase subunit	-4,52	-2,74
YJL166W	<i>QCR8</i>	Ubiquinol cyt.-c reductase subunit VIII	-4,09	-2,23



YGR183C	<i>QCR9</i>	Ubiquinol cyt.-c reductase subunit 9		-2,27
YHR001W-A	<i>QCR10</i>	Ubiquinol cyt. c oxidoreductase complex	-2,83	-2,26
YJR048W*	<i>CYC1</i>	Cytochrome-c isoform 1	-11,71	-8,76
YEL039C*	<i>CYC7</i>	Iso-2-cytochrome-c	-3,11	-2,58
YOR065W*	<i>CYT1</i>	Cytochrome c1	-6,07	-3,89
YGL187C	<i>COX4</i>	Cytochrome-c oxidase subunit IV	-3,53	-2,38
YNL052W	<i>COX5A</i>	Cytochrome-c oxidase subunit Va	-3,60	-2,20
YHR051W	<i>COX6</i>	Cytochrome-c oxidase subunit VI	-3,14	-2,38
YMR256C	<i>COX7</i>	Cytochrome-c oxidase subunit VII	-4,53	-2,10
YER141W	<i>COX15</i>	Cytochrome oxidase assembly factor		-2,03
YLL009C	<i>COX17</i>	Copper metallochaperone		-2,01
YJL116C	<i>NCA3</i>	Regulates expression of F <sub>0</sub> F <sub>1</sub> ATPase subunits	3,11	
YPR020W	<i>ATP20</i>	Mitochondrial ATP synthase subunit	-3,05	

#### Glucose fermentation

YHR094C	<i>HXT1</i>	Hexose permease	3,19	2,07
YDR345C	<i>HXT3</i>	Hexose permease	4,28	2,38
YHR092C	<i>HXT4</i>	Hexose permease	4,04	2,09
YHR096C	<i>HXT5</i>	Hexose permease	5,33	2,00
YDR343C	<i>HXT6</i>	Hexose permease	4,01	2,20
YDR342C	<i>HXT7</i>	Hexose permease	3,95	2,20
YEL069C	<i>HXT13</i>	Hexose permease	3,44	
YPL026C	<i>SKS1</i>	Serine / threonine protein kinase	2,93	
YOR374W	<i>ALD4</i>	Mitochondrial aldehyde dehydrogenase	3,64	1,90
YPL061W	<i>ALD6</i>	Acetaldehyde dehydrogenase		-2,50

#### Citric acid cycle

YLR304C	<i>ACO1</i>	Aconitase		-2,68
YNL037C	<i>IDH1</i>	Isocitrate dehydrogenase	9,91	2,13
YOR136W	<i>IDH2</i>	Isocitrate dehydrogenase	4,67	
YNR001C	<i>CIT1</i>	Citrate synthase		-2,07

#### Retrograde response

YOR374W	<i>ALD4</i>	Mitochondrial aldehyde dehydrogenase	3,54	
YML042W	<i>CAT2</i>	Carnitine O-acetyltransferase	3,1	
YCR005C	<i>CIT2</i>	Peroxisomal citrate synthase	2,89	
YPL265W	<i>DIP5</i>	Glutamate/aspartate permease	6,60	
YNL037C	<i>IDH1</i>	Isocitrate dehydrogenase	9,90	2,13
YOR136W	<i>IDH2</i>	Isocitrate dehydrogenase	4,67	
YOR222w	<i>ODC2</i>	Mitochondrial 2-oxoglutarate transporter	-4,57	
YGL026w	<i>PYC1</i>	Pyruvate carboxylase isoform	1,9	

#### Heme metabolism and heme-dependent proteins

YDR044W	<i>HEM13</i>	Coproporphyrinogen III oxidase	-1,96	
YOR176W	<i>HEM15</i>	Ferrochelatase (protoheme ferolyase)	-5,35	-3,07
YLR205C	<i>HMX1</i>	Heme oxygenase	9,0	7,27
YGR088W*	<i>CTT1</i>	Catalase T (cytosolic)	-4,48	1,85
YGR234W*	<i>YHB1</i>	Flavo-hemoglobin	-11,0	-10,72
YNL111C	<i>CYB5</i>	Cytochrome b5	-3,47	-2,66
YHR042W	<i>NCP1</i>	NADP-cytochrome P450 reductase	4,11	2,47
YJR048W*	<i>CYC1</i>	Cytochrome-c isoform 1	-11,41	-7,76
YEL039C*	<i>CYC7</i>	Iso-2-cytochrome-c	-3,11	-2,58
YPR191W*	<i>QCR2</i>	Ubiquinol cyt.-c reductase core protein 2	-4,32	-2,83
YOR065W*	<i>CYT1</i>	Cytochrome c1	-6,07	-3,89

YLR256W	<i>HAP1</i>	Heme-responsive transcription factor	4,44	1,90
YPR065W	<i>ROX1</i>	Transcriptional repressor	3,11	2,39
<b>Ergosterol biosynthesis</b>				
YNL111C	<i>CYB5</i>	Cytochrome b5	-3,47	-2,66
YMR202W	<i>ERG2</i>	C-8 sterol isomerase		-2,19
YLR056W	<i>ERG3</i>	C-5 sterol desaturase	6,80	3,18
YML126C	<i>ERG13</i>	3-hydroxy-3-methylglutaryl coenzyme A synthase		-2,11
YJL167W	<i>ERG20</i>	Farnesyl-pyrophosphate synthetase		-2,23
YER044C	<i>ERG28</i>	ER membrane protein	-2,1	-2,71
YHR042W	<i>NCP1</i>	NADP-cytochrome P450 reductase	3,51	2,47
<b>Biotin metabolism</b>				
<b>YNR056C</b>	<i>BIO5</i>	Biotin synthesis	4,33	3,06
<b>YGR065C</b>	<i>VHT1</i>	Biotin transporter	2,58	4,79
<b>Metals</b>				
YHR053C	<i>CUP1</i>	Metallothionein	3,00	
YLR220W	<i>CCC1</i>	Putative vacuolar Fe <sup>2+</sup> /Mn <sup>2+</sup> transporter	-3,43	-2,37
<b>Amino acid metabolism</b>				
YFL055W	<i>AGP3</i>	General amino acid permease	2,83	
YHR018C	<i>ARG4</i>	Argininosuccinate lyase		2,29
YPR145W	<i>ASN1</i>	Asparagine synthetase		3,23
YBR068C	<i>BAP2</i>	Branched-chain amino acid Permease		2,31
YOR303W	<i>CPA1</i>	Carbamoyl phosphate synthetase; arginine specific		3,28
YJR109C	<i>CPA2</i>	Carbamoyl phosphate synthetase		2,50
YEL009C	<i>GCN4</i>	Transcriptional activator		2,05
YDR019C	<i>GCV1</i>	Glycine decarboxylase T subunit		2,73
YMR189W	<i>GCV2</i>	Glycine decarboxylase P subunit		2,22
YAL062W	<i>GDH3</i>	NADP-glutamate dehydrogenase	3,07	
YEL046C	<i>GLY1</i>	L-threonine aldolase		2,00
YOR202W	<i>HIS3</i>	Imidazoleglycerol-phosphate dehydratase		2,60
YGL009C	<i>LEU1</i>	3-isopropylmalate isomerase	-11,3	-10,88
YCL018W	<i>LEU2</i>	Beta-isopropyl-malate dehydrogenase	8,76	4,20
YNL268W	<i>LYP1</i>	Lysine permease	2,88	2,34
YIR034C	<i>LYS1</i>	Saccharopine dehydrogenase		2,79
YNR050C	<i>LYS9</i>	Saccharopine dehydrogenase		2,02
YIL094C	<i>LYS12</i>	Homo-isocitrate dehydrogenase		2,62
YDL182W	<i>LYS20</i>	Homocitrate synthase		2,53
YOR348C	<i>PUT4</i>	Proline specific-permease		-2,78
YJR148W	<i>BAT2</i>	Branched-chain amino acid aminotransferase		2,03
YJL130C	<i>URA2</i>	Carbamoyl-phosphate synthetase	3,56	
YKR069W	<i>MET1</i>	SAM-uroporphyrinogen III transmethylase	3,94	
YJR010W	<i>MET3</i>	ATP sulfurylase		-2,15
YKL001C	<i>MET14</i>	Adenylylsulfate kinase	-5,30	-3,22
<b>Mating type reponse</b>				
YDL223C	<i>HBT1</i>	Mating projection	2,96	
YGL032C	<i>AGA2</i>	A-agglutinin binding subunit	-2,99	
YNL145W	<i>MFA2</i>	A-factor precursor	-21,5	
YPL156C	<i>PRM4</i>	Pheromone-Regulated Membrane protein	3,22	
YPL187W		Mating factor alpha	38	

YAR009C	Transposable element gene	9,13	
YAR010C	Transposable element gene	9,81	2,51
YBL005W-A	Transposable element gene	6,01	2,65
YBL005W-B	Transposable element gene	4,47	
YBL101W-A	Transposable element gene	6,82	
YBR012W-A	Transposable element gene	9,18	2,59
YCL020W	Transposable element gene	7,34	
YER138C	Transposable element gene	7,55	
YER160C	Transposable element gene	2,86	
YHR214C-B	Transposable element gene	4,17	
YJR026W	Transposable element gene	7,58	2,20
YJR027W	Transposable element gene	3,60	
YML039W	Transposable element gene	3,98	
YML040W	Transposable element gene	5,87	2,72
YML045W	Transposable element gene	4,31	2,77
YMR045C	Transposable element gene	5,48	
YMR046C	Transposable element gene	5,83	2,54
YMR050C	Transposable element gene	6,53	
YMR051C	Transposable element gene	6,84	2,52

Fold changes are given in relation to those of the wild type cultivated under the same experimental conditions. Values are averages of two biological and technical experiments including dye swaps between experiment and reference sample. Repressed genes are indicated by (-) sign. The cut-off level is 2.8 for Gal-*YAH1* and 2 for Gal-*ATM1* cells.

*AFT1* dependent genes are indicated in bold letters. *AFT2* dependent genes are underlined.

\* *HAP1* dependent genes.

### Supplementary Table SIII

Selected genes induced or repressed in cells depleted for Atm1 cultivated on SD or YPD.

ORF	Gene	Description	Average fold change	
			SD	YPD
<b>Iron regulon (Aft1p / Aft2p) / iron responsive proteins</b>				
<b>YHL040C</b>	<i>ARN1</i>	Siderophore transporter	17,36	10,19
YHL047C	<i>ARN2</i>	Siderophore transporter	30,11	18,29
<b>YEL065W</b>	<i>SIT1/</i> <i>ARN3</i>	Ferrioxamine B permease	4,06	1.4
<b>YOL158C</b>	<i>ENB1</i> <i>/ARN4</i>	Enterobactin transporter	14,52	4,46
<b>YNL259C</b>	<i>ATX1</i>	Copper metallochaperone	2,05	1.79
YDR270W*	<i>CCC2</i>	Cu(2+)-transporting ATPase	2,49	1.06
<b>YMR058W</b>	<i>FET3</i>	Cell surface ferroxidase	13,39	9,91
YMR319C	<i>FET4</i>	Iron transporter	0.25	2,62
YFL041W	<i>FET5</i>	Multicopper oxidase	2,72	2,00
<b>YDR534C</b>	<i>FIT1</i>	Retention of siderophore iron	128,55	143,09
<b>YOR382W</b>	<i>FIT2</i>	Retention of siderophore iron	94,05	79,46
<b>YOR383C</b>	<i>FIT3</i>	Retention of siderophore iron	17,64	181,76
<b>YLR214W</b>	<i>FRE1</i>	Ferric (and cupric) reductase	5,44	1,86
<b>YKL220C</b>	<i>FRE2</i>	Ferric (and cupric) reductase	4,92	3.4
<b>YOR381W</b>	<i>FRE3</i>	Ferric reductase	4,73	1,48
<b>YOR384W</b>	<i>FRE5</i>	Putative ferric reductase	3,25	1,35
YBR207W	<i>FTH1</i>	Iron transporter	2,68	1,91
<b>YER145C</b>	<i>FTR1</i>	Iron permease	9,83	4,38
<b>YLR136C</b>	<i>CTH2</i>	mRNA degradation	2,93	4,33
<b>YDR264C</b>	<i>AKR1</i>	Palmitoyl transferase	3,12	1,11
<b>YDR271C</b>		Unknown	2,31	-1,09
<b>YNR056C</b>	<i>BIO5</i>	Biotin synthesis	3,06	1.46
<b>YOR387C</b>		Unknown	-3,32	1,19
<b>YBR072W</b>	<i>HSP26</i>	Small heat shock protein	3,90	2,43
<b>YGR065C</b>	<i>VHT1</i>	Biotin transporter	4,79	2,68
<b>Fe/S protein biogenesis</b>				
YPL059W	<i>GRX5</i>	Glutathione-dependent oxidoreductase	-2,01	-1,19
<b>YPL135W</b>	<i>ISU1</i>	Scaffold protein	3,64	1,7
YOR226C	<i>ISU2</i>	Fe/S protein biogenesis	2,55	2,74
<b>Respiration</b>				
YKL148C	<i>SDH1</i>	Succinate dehydrogenase flavoprotein subunit	-3,49	-1,62
YKL141W	<i>SDH3</i>	Succinate dehydrogenase cytochrome b	-2,49	-1,89
YDR178W	<i>SDH4</i>	Succinate dehydrogenase anchor subunit	-2,50	1,3
YBL045C	<i>COR1</i>	Ubiquinol cyt.-c reductase	-2,35	-1,95
YEL024W	<i>RIP1</i>	Ubiquinol cyt.-c reductase / rieske iron-sulfur protein	-3,83	-2,56
YPR191W*	<i>QCR2</i>	Ubiquinol cyt.-c reductase core protein 2	-2,83	-1,94
YFR033C	<i>QCR6</i>	Ubiquinol cyt.-c reductase subunit	-2,12	-2,58
YDR529C	<i>QCR7</i>	Ubiquinol cyt.-c reductase subunit	-2,74	-6,11
YJL166W	<i>QCR8</i>	Ubiquinol cyt.-c reductase subunit VIII	-2,23	-3,76
YGR183C	<i>QCR9</i>	Ubiquinol cyt.-c reductase subunit 9	-2,27	-2,05
YHR001W-A	<i>QCR10</i>	Ubiquinol cyt.-c oxidoreductase complex	-2,26	-1,69



YGL187C	<i>COX4</i>	Cytochrome- <i>c</i> oxidase subunit IV	-2,38	-1,21
YNL052W	<i>COX5A</i>	Cytochrome- <i>c</i> oxidase subunit Va	-2,20	-2,23
YHR051W	<i>COX6</i>	Cytochrome- <i>c</i> oxidase subunit VI	-2,38	-3,05
YMR256C	<i>COX7</i>	Cytochrome- <i>c</i> oxidase; subunit VII	-2,10	-2,50
YGL191W	<i>COX13</i>	Cytochrome- <i>c</i> oxidase; subunit Via	-0,8	-2,76
YER141W	<i>COX15</i>	Cytochrome oxidase assembly factor	-2,03	-3,02
YLL009C	<i>COX17</i>	Copper metallochaperone	-2,01	-1,33
YJR048W*	<i>CYC1</i>	Cytochrome- <i>c</i> isoform 1	-7,76	-9,97
YEL039C*	<i>CYC7</i>	Iso-2-cytochrome- <i>c</i>	-2,58	-6,98
YOR065W*	<i>CYT1</i>	Cytochrome- <i>c</i> 1	-3,89	-4,28
YKR066C	<i>CCP1</i>	Cytochrome- <i>c</i> peroxidase	0,22	-2,18

#### Glucose fermentation

YGL256W	<i>ADH4</i>	Alcohol dehydrogenase IV	-9,71	1,03
YER073W	<i>ALD5</i>	Mitochondrial aldehyde dehydrogenase	2,03	-1,21
YPL061W	<i>ALD6</i>	Acetaldehyde dehydrogenase	-2,50	-3,76
YHR094C	<i>HXT1</i>	Hexose permease	2,17	1,23
YDR345C	<i>HXT3</i>	Hexose permease	2,38	-1,04
YHR092C	<i>HXT4</i>	Hexose permease	2,09	-1,31
YHR096C	<i>HXT5</i>	Hexose permease	2,00	1,06
YDR343C	<i>HXT6</i>	Hexose permease	2,20	1,04
YDR342C	<i>HXT7</i>	Hexose permease	2,20	-1,04
YCL040W	<i>GLK1</i>	Glucokinase	-0,1	2,24

#### Citric acid cycle

YNL037C	<i>IDH1</i>	Isocitrate dehydrogenase	2,33	2,37
YLR304C	<i>ACO1</i>	Aconitase	-2,68	-1,97
YNR001C	<i>CIT1</i>	Citrate synthase	-2,07	-1,32

#### Heme metabolism and heme-dependent proteins

YOR176W	<i>HEM15</i>	Ferrochelatase (protoheme ferrolyase)	-2,87	-1,76
YLR205C	<i>HMX1</i>	Heme-binding peroxidase	7,27	4,11
YGR234W*	<i>YHB1</i>	Flavohemoglobin	-10,72	-2,18
YNL111C	<i>CYB5</i>	Cytochrome b5	-2,66	-8,02
YHR042W	<i>NCPI/C</i> <i>PR1</i>	NADP-cytochrome P450 reductase	2,47	1,53
YJR048W*	<i>CYC1</i>	Cytochrome- <i>c</i> isoform 1	-7,76	-9,97
YEL039C*	<i>CYC7</i>	Iso-2-cytochrome- <i>c</i>	-2,58	-6,98
YPR191W*	<i>QCR2</i>	Ubiquinol cytochrome- <i>c</i> reductase core protein 2	-2,83	-1,94
YOR065W*	<i>CYT1</i>	Cytochrome <i>c</i> 1	-3,89	-4,28
YLR256W	<i>HAP1</i>	Heme-dependent transcription factor	0,58	2,56
YPR065W	<i>ROX1</i>	Transcriptional repressor	2,39	1,16

#### Ergosterol biosynthesis

YNL111C	<i>CYB5</i>	Cytochrome b5	-2,66	-8,02
YMR202W	<i>ERG2</i>	C-8 sterol isomerase	-2,19	-1,0
YLR056W	<i>ERG3</i>	C-5 sterol desaturase	2,88	2,98
YJL167W	<i>ERG20</i>	Farnesyl-pyrophosphate synthetase	-2,23	-2,50
YER044C	<i>ERG28</i>	ER membrane protein	-2,31	-1,02
YHR042W	<i>NCPI</i> <i>/CPRI</i>	NADP-cytochrome P450 reductase	2,47	1,53

<b>Metals</b>				
YHR055C	<i>CUP1-2</i>	Metallothionein	0.11	-2,00
YLR220W	<i>CCC1</i>	Transmembrane transporter; putative	-2,37	1,41
YOR316C	<i>COT1</i>	Vacuolar transporter	0.41	2,61
YHR175W	<i>CTR2</i>	Copper transporter	0.65	2,87
YOR079C	<i>ATX2</i>	Manganese-trafficking protein	0.72	2,04
<b>Amino acid metabolism</b>				
YHR018C	<i>ARG4</i>	Argininosuccinate lyase	2,29	1,2
YPR145W	<i>ASN1</i>	Asparagine synthetase	3,23	1,8
YBR068C	<i>BAP2</i>	Branched-chain amino acid Permease	2,31	1,66
YOR303W	<i>CPA1</i>	Carbamoyl phosphate synthetase; arginine specific	3,28	1,37
YJR109C	<i>CPA2</i>	Carbamoyl phosphate synthetase	2,50	1,06
YEL009C	<i>GCN4</i>	Transcriptional activator	2,05	1,94
YDR019C	<i>GCV1</i>	Glycine decarboxylase T subunit	2,73	1,82
YMR189W	<i>GCV2</i>	Glycine decarboxylase P subunit	2,22	1,43
YOR375C	<i>GDH1</i>	Glutamate dehydrogenase	-0,29	-2,33
YEL046C	<i>GLY1</i>	L-threonine aldolase	2,00	1,37
YOR202W	<i>HIS3</i>	Imidazoleglycerol-phosphate dehydratase	2,60	1,15
YGL009C	<i>LEU1</i>	3-isopropylmalate isomerase	-10,88	-8,08
YCL018W	<i>LEU2</i>	Beta-isopropyl-malate dehydrogenase	4,20	1,74
YNL268W	<i>LYP1</i>	Lysine permease	2,24	1,85
YIR034C	<i>LYS1</i>	Saccharopine dehydrogenase	2,79	2
YNR050C	<i>LYS9</i>	Saccharopine dehydrogenase	2,02	1,69
YIL094C	<i>LYS12</i>	Homo-isocitrate dehydrogenase	2,62	3,25
YDL182W	<i>LYS20</i>	Homocitrate synthase	2,53	2,82
YOR348C	<i>PUT4</i>	Proline specific-permease	-2,78	-1,7
YHR208W	<i>BAT1</i>	Transaminase	-0,45	-2,41
YJR148W	<i>BAT2</i>	Branched-chain amino acid aminotransferase	2,03	2,15
Yer175C	<i>TMT1</i>	Trans-aconitate methyltransferase	5,84	4,60
YJR010W	<i>MET3</i>	ATP sulfurylase	-2,15	-1,0
YKL001C	<i>MET14</i>	Adenylylsulfate kinase	-3,22	-1,66
<b>Mating type reponse</b>				
YAR010C		Transposable element gene	2,51	1,7
YBL005W-A		Transposable element gene	2,65	-1,03
YBR012W-A		Transposable element gene	2,59	1,67
YJR026W		Transposable element gene	2,50	2,31
YML040W		Transposable element gene	2,72	1,26
YML045W		Transposable element gene	2,77	1,65
YMR046C		Transposable element gene	2,54	1,69
YMR051C		Transposable element gene	2,52	2,2

Fold changes are given in relation to those of the wild type cultivated under the same experimental conditions. Values are averages of two biological and technical experiments including dye swaps between experiment and reference sample. Repressed genes are indicated by (-) sign. The cut-off level is 2.

*AFT1* dependent genes are indicated in bold letters. *AFT2* dependent genes are underlined.

\* *HAP1* dependent genes.

**Supplementary Table SIV: Yeast strains used in this study.**

Strain	Genotype	Method of Generation	Source/Reference
W303-1A	<i>MAT<math>\alpha</math>; ura3-1; ade2-1; trp1-1; his3-11,15; leu2-3,112</i>		(1)
W303-1B	<i>MAT<math>\alpha</math>; ura3-1; ade2-1; trp1-1; his3-11,15; leu2-3,112</i>		(1)
BY4742	<i>MAT<math>\alpha</math>; his3<math>\Delta</math>1; leu2<math>\Delta</math>0; lys2<math>\Delta</math>0; ura3<math>\Delta</math>0</i>	obtained from Euroscarf	(2)
Gal-ATM1	W303-1B, <i>pATM1::GAL1-10-LEU2</i>	gene replacement (pYEP51-Gal-ATM1)	(3)
Gal-ATM1, <i>hmx1<math>\Delta</math></i>	W303-1B, <i>pATM1::GAL1-10-LEU2; hmx1::HIS3</i>	PCR fragment (pFA6a-HIS3)	this work
Gal-NBP35	W303-1A, <i>pNBP35::GAL1-10-HIS3</i>	PCR fragment (pFA6a-HIS3-Gal) (4)	(5)
Gal-YAH1	W303-1B, <i>pYAH1::GAL1-10-LEU2</i>	gene replacement (pYEP51-Gal-YAH1)	(6)
Gal-YAH1, <i>hmx1<math>\Delta</math></i>	W303-1B, <i>pYAH1::GAL1-10-LEU2; hmx1::HIS3</i>	PCR fragment (pFA6a-HIS3)	this work
Gal-SSQ1	W303-1A <i>pSSQ1::GAL1-10-HIS3</i>	PCR fragment (pFA6a-HIS3-Gal) (4)	(7)
Gal-HEM15	W303-1A, <i>pHEM15::GAL1-10-HIS3</i>	PCR fragment (pFA6a-HIS3-Gal) (4)	this work
Gal-GRX5	W303-1A, <i>pGRX5::GAL1-10-HIS3</i>	PCR fragment (pFA6a-HIS3-Gal) (4)	(7)
Gal-YFH1	W303-1A, <i>pYFH1::GAL1-10-HIS3</i>	PCR fragment (pFA6a-HIS3-Gal) (4)	(4)
<i>aco1<math>\Delta</math></i>	W303-1A, <i>aco1::HIS3</i>	PCR Fragment (pFA6a-HIS3MX6)	this work
<i>cth2<math>\Delta</math></i>	BY4741; <i>cth2::kanMX6</i>	PCR fragment (pFA6a-KanMX4)	Euroscarf
<i>cyt2<math>\Delta</math></i>	W303-1A, <i>cyt2::LEU2</i>	gene replacement	(8)
<i>hmx1<math>\Delta</math></i>	W303-1A, <i>hmx1::HIS3</i>	PCR fragment (pFA6a-HIS3)	this work
<i>sod1<math>\Delta</math></i>	W303-1A, <i>sod1::LEU2</i>	PCR fragment(9) (pUG73)	this work

Gene disruptions and promoter exchanges were generated by PCR-based gene replacement and verified by PCR as described previously (4).

1. Mortimer, R. K., and Johnston, J. R. (1986) *Genetics* **113**(1), 35-43
2. Brachmann, C. B., Davies, A., Cost, G. J., Caputo, E., Li, J., Hieter, P., and Boeke, J. D. (1998) *Yeast* **14**(2), 115-132
3. Kispal, G., Csere, P., Guiard, B., and Lill, R. (1997) *FEBS Lett* **418**(3), 346-350
4. Muhlenhoff, U., Richhardt, N., Ristow, M., Kispal, G., and Lill, R. (2002) *Hum Mol Genet* **11**(17), 2025-2036
5. Hausmann, A., Aguilar Netz, D. J., Balk, J., Pierik, A. J., Muhlenhoff, U., and Lill, R. (2005) *Proc Natl Acad Sci U S A* **102**(9), 3266-3271
6. Lange, H., Kaut, A., Kispal, G., and Lill, R. (2000) *Proc Natl Acad Sci U S A* **97**(3), 1050-1055
7. Muhlenhoff, U., Gerber, J., Richhardt, N., and Lill, R. (2003) *Embo J* **22**(18), 4815-4825
8. Steiner, H., Zollner, A., Haid, A., Neupert, W., and Lill, R. (1995) *J Biol Chem* **270**(39), 22842-22849
9. Gueldener, U., Heinisch, J., Koehler, G. J., Voss, D., and Hegemann, J. H. (2002) *Nucleic Acids Res* **30**(6), e23